sustainability

MDPI

Article

Optimal Allocation of Photovoltaic Distributed Generations in Radial Distribution Networks

Samson Oladayo Ayanlade [1,*], Funso Kehinde Ariyo [2], Abdulrasaq Jimoh [2], Kayode Timothy Akindeji [3], Adeleye Oluwaseye Adetunji [4], Emmanuel Idowu Ogunwole [5] and Dolapo Eniola Owolabi [6]

1 Department of Electrical and Electronic Engineering, Faculty of Engineering and Technology, Lead City University, Ibadan 200255, Nigeria
2 Department of Electronic and Electrical Engineering, Faculty of Technology, Obafemi Awolowo University, Ile-Ife 220101, Nigeria; ariyofunso@oauife.edu.ng (F.K.A.); jimohabdulrasaq@gmail.com (A.J.)
3 Smart Grid Research Center, Department of Electrical Power Engineering, Faculty of Engineering and the Built Environment, Durban University of Technology, Durban 4000, South Africa; kayodea@dut.ac.za
4 Department of Electrical and Electronic Engineering, Faculty of Engineering and Environmental Sciences, Osun State University, Osogbo 210001, Nigeria; tunjiat17@gmail.com
5 Department of Electrical, Electronic and Computer Engineering, Cape Peninsula University of Technology, Cape Town 7535, South Africa; 221597999@mycput.ac.za
6 Department of Electronic and Electrical Engineering, Faculty of Engineering and Technology, Ladoke Akintola University of Technology, Ogbomoso 210214, Nigeria; owolabidolapo343@gmail.com
* Correspondence: samson.ayanlade@lcu.edu.ng; Tel.: +234-8062786683

Abstract: Photovoltaic distributed generation (PVDG) is a noteworthy form of distributed energy generation that boasts a multitude of advantages. It not only produces absolutely no greenhouse gas emissions but also demands minimal maintenance. Consequently, PVDG has found widespread applications within distribution networks (DNs), particularly in the realm of improving network efficiency. In this research study, the dingo optimization algorithm (DOA) played a pivotal role in optimizing PVDGs with the primary aim of enhancing the performance of DNs. The crux of this optimization effort revolved around formulating an objective function that represented the cumulative active power losses that occurred across all branches of the network. The DOA was then effectively used to evaluate the most suitable capacities and positions for the PVDG units. To address the power flow challenges inherent to DNs, this study used the Newton–Raphson power flow method. To gauge the effectiveness of DOA in allocating PVDG units, it was rigorously compared to other metaheuristic optimization algorithms previously documented in the literature. The entire methodology was implemented using MATLAB and validated using the IEEE 33-bus DN. The performance of the network was scrutinized under normal, light, and heavy loading conditions. Subsequently, the approach was also applied to a practical Ajinde 62-bus DN. The research findings yielded crucial insights. For the IEEE 33-bus DN, it was determined that the optimal locations for PVDG units were buses 13, 25, and 33, with recommended capacities of 833, 532, and 866 kW, respectively. Similarly, in the context of the Ajinde 62-bus network, buses 17, 27, and 33 were identified as the prime locations for PVDGs, each with optimal sizes of 757, 150, and 1097 kW, respectively. Remarkably, the introduction of PVDGs led to substantial enhancements in network performance. For instance, in the IEEE 33-bus DN, the smallest voltage magnitude increased to 0.966 p.u. under normal loads, 0.9971 p.u. under light loads, and 0.96004 p.u. under heavy loads. These improvements translated into a significant reduction in active power losses—61.21% under normal conditions, 17.84% under light loads, and 33.31% under heavy loads. Similarly, in the case of the Ajinde 62-bus DN, the smallest voltage magnitude reached 0.9787 p.u., accompanied by an impressive 71.05% reduction in active power losses. In conclusion, the DOA exhibited remarkable efficacy in the strategic allocation of PVDGs, leading to substantial enhancements in DN performance across diverse loading conditions.

Keywords: active power loss; distributed generation; voltage profile; reactive power loss; PVDG; dingo optimization algorithm

check for updates

Citation: Ayanlade, S.O.; Ariyo, F.K.; Jimoh, A.; Akindeji, K.T.; Adetunji, A.O.; Ogunwole, E.I.; Owolabi, D.E. Optimal Allocation of Photovoltaic Distributed Generations in Radial Distribution Networks. *Sustainability* **2023**, *15*, 13933. https://doi.org/10.3390/su151813933

Academic Editors: Pablo García Triviño and Mohamed A. Mohamed

Received: 6 July 2023
Revised: 11 September 2023
Accepted: 14 September 2023
Published: 19 September 2023

Copyright: © 2023 by the authors. Licensee MDPI, Basel, Switzerland. This article is an open access article distributed under the terms and conditions of the Creative Commons Attribution (CC BY) license (https://creativecommons.org/licenses/by/4.0/).

1. Introduction

The power system holds great significance in stimulating the economy of a nation. It consists of generation, transmission, and distribution systems, which are separated due to deregulation [1,2]. Among these components, the distribution system faces numerous technical challenges, including poor voltage profiles, huge losses, and voltage collapse [3]. Extensive efforts have been made by power system engineers and researchers to address these issues and enhance the effectiveness of distribution networks (DNs). One successful approach is the deployment of distributed generation (DG). DG encompasses four types: types 1, 2, 3, and 4. These DG types have proven effective in reducing power losses in DNs. However, due to the growing demand for green energy, type 1 DG, specifically, photovoltaic distributed generation (PVDG), is widely used for its greenhouse gas (GHG)-free operation [4]. PVDG injects active power into the DNs, thereby improving network performance and power delivery capability [5,6]. Additionally, it alleviates the burden on the DNs caused by load demands, enhancing overall reliability.

However, proper allocation of DG is crucial to achieving the desired objectives when deploying DG on DNs. Researchers have extensively developed and utilized metaheuristic optimization algorithms to address the challenges associated with optimum allocation problems in DGs. Previous studies have explored optimal DG deployment, specifically focusing on PVDG, to optimize operational performance. For instance, Ref. [7] used the Archimedes optimization algorithm (AOA), motivated by physical concepts, to determine the appropriate positions and capacities of solar photovoltaic (PV) systems in distribution systems. Their study aimed to reduce grid reliance and greenhouse gas emissions by defining the search space using loss sensitivity parameters and applying AOA to identify suitable solar PV system locations and sizes. Similarly, Albadi et al. [8] investigated the appropriate placement of PVs in a DN utilizing particle swarm optimization (PSO) and the genetic algorithm (GA). Their objective was to minimize transmission loss while improving voltage profiles using the Masirah Island network in Oman as a case study. Ali et al. [9] investigated the utilization of PV and wind turbine (WT) systems as DGs within radial DNs. They used white shark optimization (WSO) to obtain the optimum location and sizes of these systems using a balance between exploration and exploitation for global optimization. The study used IEEE 33-, 69-, and 85-bus DNs to evaluate the efficacy of the WSO approach. The findings revealed that WSO effectively reduced power losses, improved voltage profiles, and outperformed other strategies. Increasing the number of units resulted in significant loss reductions (up to 93.52% for WT and 52.267% for PV), along with substantial annual cost savings. Moreover, the addition of PV and WT units led to notable enhancements in voltage profiles. The practical implementation of the WSO approach was validated by considering constraints and operational requirements.

Furthermore, Khenissi et al. [10] studied the optimum capacity and allocation of PVDGs in a modified IEEE 14-bus DN. They used PSO and the GA as optimization approaches to diminish overall power loss and boost voltage and frequency profiles. Their research included two scenarios to examine the impact of PV integration, load consumption fluctuations, and atmospheric conditions on size optimization. The efficacy of PSO was also explored by Albadi et al. [11], who conducted a study to find the ideal position and capacity of solar PVs in a DN. The Masirah Island network in Oman served as the testbed. In another study, Ali et al. [12] proposed the ant lion optimization algorithm (ALOA) to optimize the placement and scaling of DG renewable resources in DNs. They utilized loss sensitivity parameters to identify potential DG implementation sites and used the ALOA to determine DG locations and sizes on selected buses, testing their method on a 69-bus radial DN. Ahmed et al. [13] investigated the performance of DNs with single and multiple PV-based DGs at varying load levels. They aimed to diminish the overall loss and boost the network performance by determining the ideal position and DG capacity in the DN. Their approach utilized the augmented grey wolf optimizer and loss sensitivity factor and was validated on an IEEE 69-bus distribution system, demonstrating its effectiveness.

Ahmadi et al. [14] conducted a research study on integrating renewable energy resources in the power network of Afghanistan, specifically focusing on rooftop solar PV as DG. They used a GA with a Newton–Raphson approach to optimize the capacity and placement of solar PV in a 162-bus electric DN in Kabul. The objective was to reduce losses and voltage deviation, thereby reducing dependence on imported power and improving system performance. The proposed method was simulated using MATLAB 2018a software to evaluate system performance under various PV allocation scenarios. Khasanov et al. [15] introduced an algorithm known as artificial ecosystem-based optimization-opposition-based learning (AEO-OBL) as an enhanced version of the artificial ecosystem-based optimization (AEO) algorithm. The primary objective of AEO-OBL was to optimize the DG allocation in DNs to diminish the overall power losses. The algorithm considered the unpredictable character of renewable DGs and integrated five strategies to prevent local optima. In the study, the loss sensitivity index was used to determine appropriate buses for integrating DGs into the DN. AEO-OBL was compared with other optimization algorithms from the existing literature. Experimental results were obtained using the IEEE 33-bus and 85-bus DNs, demonstrating the superior performance of AEO-OBL in solving the optimal DG allocation problem in DNs.

Purlu and Belgin [16] presented two metaheuristic methods, the GA and PSO, for the purpose of determining the optimal positions, power factor (PF), and capacities of DGs within a DN. The goal was to integrate renewable energy sources into the system to achieve carbon neutrality by 2050. Unlike previous studies, this research considered seasonal uncertainties in generation and consumption to diminish power losses and voltage violations. The algorithms were tested on a 33-bus DN with various constraints. The results showed that operating DG sources at optimal PFs yielded better outcomes than operating them at a unity PF. The results indicated that wind turbines exhibited higher effectiveness compared with PV systems and demonstrated a performance level comparable to conventional power sources with controllable power output. PSO outperformed the GA with regard to solution quality, convergence speed, and runtime, showcasing its superior performance. Tukkee et al. [17] addressed the competition among electrical power companies to provide superior services that balanced stability and environmental benefits. They highlighted the integration of solar PVs as a solution for improving bus voltage profiles and minimizing system losses. The authors proposed a firefly algorithm (FA) and utilized a fast voltage stability index to determine suitable bus locations for solar PV penetration. The algorithm aimed to boost the voltage magnitudes and diminish losses. Experiments on the IEEE 33-bus DN compared the FA method with the GA approach. The FA method achieved a 6.46% minimization in losses, slightly outperforming the GA technique's 6% reduction. Furthermore, the FA method demonstrated an enhancement in the network's voltage profile.

Mubarak et al. [18] examined the growing need for dependable power supplies within the Industrial Revolution 4.0. They highlighted the significance of effective planning in electrical power systems to accommodate increasing loads, integrate DGs, ensure optimum operation during contingencies, and adhere to DN constraints. Nonetheless, these challenges escalate the complexity of distribution system planning due to technical limitations and a vast search space. To address these concerns, the researchers introduced a strategy using a hybrid FA-PSO to discover an optimal solution for expansion planning. The effectiveness of this approach was evaluated using IEEE 33-bus and 69-bus DNs, which revealed that incorporating DGs with optimized capacity and placement significantly diminished investment and power loss costs. Comparative assessments were also carried out to establish the method's efficacy when compared to existing models documented in the literature. Khan et al. [19] carried out a study that addressed the challenges encountered by the power distribution system, which included power losses, voltage deviations, and reliability issues. To tackle these challenges and meet the rising electricity demand, the researchers proposed an optimal allocation strategy for DGs using metaheuristic optimization algorithms. The study introduced an objective function and used the honey badger algorithm (HBA) to

determine the appropriate capacities of four categories of DGs. A comparison was made with the GWO and WOA. The main objective was to enhance the voltage bus magnitudes and mitigate losses in the IEEE 33-bus and 69-bus DNs. Their simulation findings showed that the HBA outperformed the GWO and WOA, achieving accurate and optimal outcomes within only one iteration for the IEEE 33-bus DN and two iterations for the 69-bus DN. Furthermore, the losses were minimized in both the IEEE 33-bus and 69-bus DNs. Jamil Mahfoud et al. [20] used a novel approach to address the optimal planning of distributed generators (OPDGs) in radial distribution systems (RDSs). This approach involved combining the original differential evolution algorithm (DE) with the search mechanism of Lévy flights (LFs) to create a new algorithm called the quasi-oppositional differential evolution Lévy flights algorithm (QODELFA). Additionally, the quasi-opposition-based learning concept (QOBL) was used to generate the initial population for QODELFA. The study focused on optimizing three objective functions: minimizing active power loss, improving voltage profiles, and enhancing voltage stability while adhering to various operational constraints. To assess the effectiveness of QODELFA, the algorithm was tested on the IEEE 33-bus, 69-bus, and 118-bus systems, and its performance was compared with existing methods. The results of these comparisons demonstrated that the proposed QODELFA outperformed many established methods, establishing it as a robust and efficient solution for solving the OPDG problem.

Nowdeh et al. [21] used a novel approach to address loss reduction and reliability enhancement in radial distribution systems with the strategic integration of renewable energy sources such as photovoltaic panels (PVs) and wind turbines (WTs). Their objective was to minimize losses and improve reliability, measured using energy not supplied (ENS). To achieve this, they introduced the multi-objective hybrid teaching–learning-based optimization–grey wolf optimizer (MOHTLBOGWO), a powerful evolutionary algorithm with rapid convergence and the ability to avoid local optima. The proposed methodology was applied in both single-objective and multi-objective forms to the IEEE radial distribution networks with 33 and 69 buses. The results indicated that the multi-objective optimization approach provided a more accurate representation of network performance by considering various objective indices, outperforming the single-objective method. Additionally, the study revealed that the proposed method exhibited superior convergence speed and lower convergence tolerance compared with other methods like TLBO and GWO, resulting in enhanced loss reduction, improved reliability, increased net savings, and surpassing previous research findings. Furthermore, dispersing the size and location of distributed renewable generation resources led to even greater loss reduction and reliability enhancement.

While previous studies have explored the optimum allocation of PVDG using various metaheuristic techniques, there is still potential for further advancements to enhance DN performance and decrease active power losses. This research introduces a unique approach using the dingo optimization algorithm (DOA), a novel optimization approach, to allocate PVDG within DNs. The effectiveness of the DOA was evaluated by allocating PVDGs on an IEEE 33-bus network under different loading conditions and subsequently validated using a practical Nigerian DN. The novelty of this research article lies in its exploration of the DOA as a novel and efficient approach for allocating PVDG units on DNs. Using DOA's adaptive search strategy, fast convergence rate, and ability to handle complex constraints, this study demonstrates the algorithm's potential as a promising and competitive bio-inspired optimization tool for effectively integrating PVDG units into DNs. This research article's primary contributions to the body of knowledge can be summarized as follows:

- Introducing the DOA as a powerful tool for optimal allocation of PVDG in DNs, thereby advancing power system optimization techniques.
- Applying the DOA to a practical Ajinde 62-bus Nigerian DN to demonstrate its real-world effectiveness in PVDG allocation.
- Providing empirical evidence of the DOA's performance in PVDG allocation, thereby contributing to the existing literature on DN optimization.

- Advancing understanding of the PVDG effect on DN performance.
- Establishing a foundation for future research on the application of DOA and other optimization algorithms for PVDG allocation in various DN configurations and scenarios.
- Offering insights and recommendations for optimal location and capacity of PVDG to enhance DN performance and reduce environmental impact.

In essence, the aim of this study is to contribute to the field of power system optimization and promote the transition toward sustainable and efficient DNs.

The structure of this article is as follows: Section 2 develops the objective function for this study. In Section 3, an exposition of the DOA methodology was presented, offering a thorough and in-depth understanding of its principles and intricacies. The results and discussion are presented in Section 4, and the conclusions are provided in Section 5.

2. Problem Formulation

2.1. Objective Function

The primary objective of deploying PVDG on DNs is to reduce the overall active loss, which represents the cumulative active loss across all branches of the network. In this study, the optimization problem focuses on diminishing the cumulative active power loss as the objective function (*OF*), which is expressed as:

$$OF_{\min} = \sum_{i}^{n_b} |I_i|^2 R_i \tag{1}$$

where n_b = overall network lines, R_i = ith line resistance, and $|I_i|$ = ith line current.

2.2. Equality Constraints

The subsequent subsections provide a detailed discussion of the equality and inequality constraints that the objective function is subjected to.

Power Flow Balance and Generation

These equations, denoted as (2) and (3), represent the essential components of the network's active and reactive power flows. Equation (2) captures the dynamic behavior of active power flow, while Equation (3) provides a quantitative representation of reactive power flow.

$$P_{Gi} = P_{Di} + \sum_{j=1}^{n_b} |V_i||V_j|\left[G_{ij}\cos\theta_{ij} + B_{ij}\sin\theta_{ij}\right] \tag{2}$$

$$Q_{Gi} = Q_{Di} + \sum_{j=1}^{n_b} |V_i||V_j|\left[G_{ij}\sin\theta_{ij} - B_{ij}\cos\theta_{ij}\right] \tag{3}$$

where V_i and V_j = bus voltage values, P_{Gi} and P_{Di} = active power supplied and demanded, respectively, Q_{Gi} and Q_{Di} = reactive power supplied and demanded, respectively, and G_{ij} and B_{ij} = line conductance and susceptance, respectively.

2.3. Inequality Constraints

These specified limits encompass the voltage thresholds applicable to all buses within the network in addition to the restrictions imposed on the PVDG units.

2.3.1. Voltage Limits

Equation (4) defines the upper and lower voltage limits, encapsulating the precise boundaries within which the voltage levels should operate.

$$V_{\min} \le V_i \le V_{\max} \tag{4}$$

where $V_{\min}$ and $V_{\max}$ = minimum and maximum voltage magnitudes, respectively.

2.3.2. Photovoltaic Distributed Generation Limits

The optimal operation of PVDG units necessitates adherence to specific operational boundaries, defined by the lower and upper limits, as expressed in Equation (5).

$$PVDG_{(\min)} \leq PVDG \leq PVDG_{(\max)} \tag{5}$$

where $PVDG_{\min}$ and $PVDG_{\max}$ = minimum and maximum active power magnitudes, respectively.

3. Dingo Optimization Algorithm

The DOA draws inspiration from the social dynamics and hunting strategies of dingoes, which are known for their cleverness and social dynamics [22]. Dingoes live in packs consisting of 12 to 15 members, with an alpha serving as the dominant and most powerful individual within the pack. Subordinate members, including betas, submit to the alpha's authority. The pack includes scouts who are responsible for monitoring the surroundings and alerting the group to potential threats or situations. Dingoes exhibit a unique hunting behavior characterized by coordinated actions such as pursuing, pestering, surrounding, and attacking prey. The DOA algorithm leverages these aspects of dingo behavior to optimize the allocation of resources in a manner that resembles the strategic coordination of a dingo pack. By incorporating elements of dingo social organization and hunting behavior, the DOA algorithm demonstrates its adaptability and effectiveness in solving optimization problems in various domains, including power system optimization. This utilization of dingo behavior adds a novel and valuable dimension to the field of optimization algorithms.

3.1. Mathematical Modeling of the Dingo Optimization Algorithm

The DOA uses a mathematical model that simulates the circling, hunting, attacking, and searching behaviors observed in the natural behavior of animals, such as dingoes, during the optimization process [23]. This model allows the DOA to mimic the adaptive and efficient strategies utilized by dingoes in their pursuit of prey. By incorporating these natural behaviors into the algorithm, the DOA demonstrates enhanced performance and effectiveness in solving optimization problems in various domains.

3.1.1. Encircling

The encircling behavior of dingoes, which involves the strategic positioning and coordination of the pack members, is modeled using mathematical Equations (6)–(10).

$$\vec{D}_c = \left| \vec{A} \cdot \vec{P}_p(x) - \vec{P}(x) \right| \tag{6}$$

$$\vec{P}(i+1) = \vec{P}_p(i) - \vec{B} \cdot \vec{D}(d) \tag{7}$$

$$\vec{A} = 2 \cdot \vec{a}_1 \tag{8}$$

$$\vec{B} = 2\vec{b} \cdot \vec{a}_2 - \vec{b} \tag{9}$$

$$\vec{b} = 3 - \left(I * \left(\frac{3}{I_{\max}} \right) \right) \tag{10}$$

where $\vec{D}_d$ = separation between the prey and dingo, $\vec{P}_P$ and $\vec{P}$ = prey and dingo position vectors, respectively, $\vec{A}$ = coefficient vector, $\vec{B}$ = coefficient vector, $\vec{a}_1$ = random vector in [0, 1], $\vec{a}_2$ = random vector in [0, 1], $\vec{b}$ = variable that falls linearly from 3–0, and I = 1, 2, 3,. . ., $I_{\max}$.

These equations capture the essence of how dingoes surround their prey and work together as a cohesive unit. By applying these mathematical models, the effectiveness of this encircling behavior in the context of optimization algorithms can be simulated and analyzed [24].

3.1.2. Hunting

In the context of optimization algorithms, the prey's position computation in the search space, representing the optimum solution, is typically not available to individual agents. However, in the DOA algorithm, it is assumed that all members of the pack possess knowledge of potential prey locations, which is incorporated into the mathematical representation of the dingo hunting strategy. In the hunting behavior of dingoes, the alpha dingo takes charge of the hunt, but other members, such as beta and subordinate dingoes, may also participate. In the DOA, the positions of the two best search agents obtained so far are selected for reference. The remaining dingoes update their positions based on the best search agent location, as described in Equations (11)–(16).

$$\vec{D}_\alpha = \left| \vec{A}_1 \cdot \vec{P}_\alpha - \vec{P} \right| \tag{11}$$

$$\vec{D}_\beta = \left| \vec{A}_2 \cdot \vec{P}_\beta - \vec{P} \right| \tag{12}$$

$$\vec{D}_o = \left| \vec{A}_3 \cdot \vec{P}_o - \vec{P} \right| \tag{13}$$

$$\vec{P}_1 = \left| \vec{P}_\alpha - \vec{B} \cdot \vec{D}_\alpha \right| \tag{14}$$

$$\vec{P}_2 = \left| \vec{P}_\beta - \vec{B} \cdot \vec{D}_\beta \right| \tag{15}$$

$$\vec{P}_3 = \left| \vec{P}_o - \vec{B} \cdot \vec{D}_o \right| \tag{16}$$

These equations capture the essence of the hunting strategy within the DOA, aligning with the notion that dingoes in a pack coordinate their movements based on the actions of the alpha and the information available from other members of the group. By modeling this aspect, the DOA introduces a unique mechanism for optimizing the search process, mirroring the collective intelligence and cooperation observed in dingo packs during hunting activities. The intensity of each dingo is determined using Equations (17)–(19).

$$\vec{I}_a = \log\left(\frac{1}{F_\alpha - (1E - 100)} + 1 \right) \tag{17}$$

$$\vec{I}_\beta = \log\left(\frac{1}{F_\beta - (1E - 100)} + 1 \right) \tag{18}$$

$$\vec{I}_o = \log\left(\frac{1}{F_o - (1E - 100)} + 1 \right) \tag{19}$$

where F_α and F_β = α- and β-dingo fitness values, respectively, and F_o = other dingo fitness value.

These equations capture the mathematical calculations involved in evaluating the dingo intensities within the DOA.

3.1.3. Attacking Prey

After completing the hunt, the dingo proceeds to attack the prey if no position update is required. To formulate this behavior mathematically, the value of the variable $\vec{b}$ is linearly decreased. It is important to note that the range of change in the variable $\vec{D}_\alpha$ is also reduced by $\vec{b}$. In each iteration, the value of $\vec{b}$ is gradually decreased from 3 to 0. The variable $\vec{D}_\alpha$ is a random variable that takes values within the interval $[-3b, 3b]$, where b represents a specific parameter. As $\vec{b}$ decreases from 3 to 0, the range of random values for $\vec{D}_\alpha$ becomes narrower. For instance, when $\vec{D}_\alpha$ takes random values within the range $[-1, 1]$, the subsequent location of a search agent can lie anywhere between its current position and the prey's position. By incorporating these mathematical adjustments, the DOA algorithm simulates the dingo's decision-making process during the hunt, gradually reducing the range of possible movements as the hunting progresses. This approach enhances the search agent's exploration and exploitation capabilities, allowing them to converge toward optimal solutions more effectively.

3.1.4. Searching

Dingoes use the position of the group to locate prey and actively pursue and attack them. In the DOA, random values represented by $\vec{B}$ are used, with values smaller than -1 indicating prey moving away from the hunter and values larger than 1 indicating the pack approaching the prey. This approach enables global scanning of targets in the DOA. Another component, $\vec{A}$, promotes exploration. In Equation (8), $\vec{A}$ generates a random integer between 0 and 3, accommodating variable prey weights. The DOA is a probabilistic variable, with the vector ≤ 1 preceding the vector ≥ 1, allowing the analysis of the influence of the gap described in Equation (7).

3.2. Application of the Dingo Optimization Algorithm for Optimal DG Allocation

1. Initialize the population of dingo agents with haphazard locations and velocities within the search area.
2. Assess the fitness of each dingo agent by applying a fitness function that takes into account the network's performance after the DGs have been allocated.
3. Identify the dingo agent with the best fitness value as the global best solution.
4. Update the position and each dingo agent's velocity depending on its own knowledge and the global best solution.
5. Apply boundary constraints to ensure that the updated positions of the dingo agents remain within the feasible region.
6. Evaluate the fitness of each updated dingo agent.
7. Compare the fitness values of the updated dingo agents with their previous fitness values and modify the personal best solution for each agent.
8. Modify the global best solution if a dingo agent finds a better solution.
9. Repeat steps 4–8 until the termination criteria are met.
10. Choose the best dingo agent as the final solution and allocate the DGs to the radial DN based on their positions.

A flowchart illustrating the process is presented in Figure 1. In the allocation of PVDGs within the IEEE 33-bus and Ajinde 62-bus DNs using the DOA, several parameters were selected. These parameters included the following typical values:

1. Population Size: A typical population size of around 1000 individuals was chosen to represent potential solutions.

2. Maximum Generations: The algorithm was allowed to evolve over a maximum of 100 generations to find optimal solutions.
3. Crossover Rate: A moderate crossover rate of 0.7 was used to balance exploration and exploitation.
4. Mutation Rate: A typical mutation rate of 0.1 was set to introduce diversity into the population.
5. Selection Pressure: The selection pressure, which determines the probability of selecting fitter individuals, was set to a standard value of 2.
6. Convergence Criteria: Convergence was typically considered to be achieved when the improvement in the objective function (active power losses) reached a predefined threshold, often set at 1% or lower.

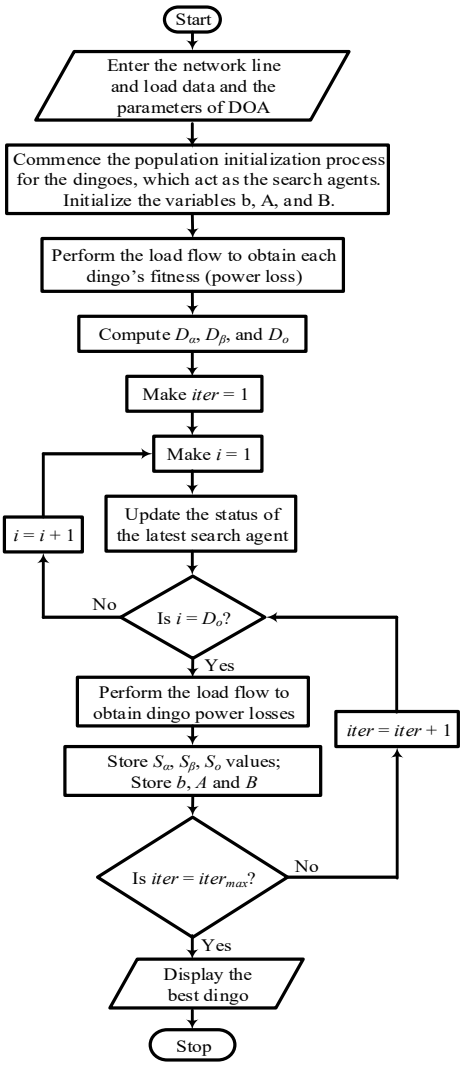


Figure 1. Implementation of the DOA for PVDG allocation.

These parameter values were carefully selected and applied in the DOA to efficiently allocate PVDGs in the IEEE 33-bus and Ajinde 62-bus DNs.

4. Results and Discussion

A novel and technically advanced approach, the DOA method, was used to address the optimal placement and sizing of PVDG units in power DNs under study. The implementation of the DOA technique was carried out using the robust MATLAB package, harnessing its powerful computational capabilities. To assess the effectiveness and versatility of the DOA approach, extensive evaluations were conducted on both the IEEE 33-bus

and the practical Ajinde 62-bus Nigerian DNs. The IEEE 33-bus network served as the initial testing ground, where the DOA's performance was scrutinized under various load conditions, namely, normal, light, and heavy loads. In the context of this study, normal load represented the standard operating conditions of the network. The light and heavy load scenarios were obtained by systematically reducing and elevating the network loads by 50% and 10%, respectively. The DOA methodology was then assessed under these distinct load conditions to validate its reliability and adaptability across different operational scenarios. The key variables used in the DOA analysis were population size (D_n = 1000) and maximum number of iterations ($iter_{max}$ = 200). These parameters were thoughtfully chosen to strike an optimal balance between computational efficiency and solution accuracy. The simulations were performed using the industry-standard MATLAB/SIMULINK software package, which facilitated rigorous testing and validation of the DOA approach. Once successfully validated on the IEEE 33-bus network, the DOA technique was further scrutinized and verified on the practical Ajinde 62-bus Nigerian DN. This practical DN provided a more complex and challenging environment, allowing the DOA method to showcase its applicability and effectiveness in addressing real-world DN scenarios.

4.1. IEEE 33-Bus Network

The aim of this technical study conducted on the IEEE 33-bus DN was to improve the overall performance of the network under varying load conditions by strategically deploying PVDG units. The network consists of 33 buses and 31 lines, and comprehensive line and load data were sourced from [25]. The network's configuration is visually represented in Figure 2, showcasing its single-line diagram. To evaluate the effectiveness of DOA-optimized PVDG integration, simulations were conducted for three different loading scenarios on the network: normal, light, and heavy loads. Convergence in the power flow simulation process was successfully achieved after three iterations for each loading condition. The outcomes of the simulations are presented in Table 1. Table 1 highlights the optimal locations for PVDG deployment within the IEEE 33-bus DN. The optimal buses for PVDG placement were identified as buses 13, 25, and 33. Also, Table 1 reveals the corresponding sizes of the PVDG units deployed at these locations, with capacity values of 833, 532, and 866 kW for buses 13, 25, and 33, respectively. The convergence curve for DOA is illustrated in Figure 3. As illustrated in Figure 3, despite the initial setting of a maximum limit of 100 generations for the algorithm's evolution, the simulation results revealed consistent convergence to optimal solutions in approximately 21 iterations. This efficiency in reaching optimal outcomes at a substantially reduced iteration count highlighted the algorithm's effectiveness. Consequently, there was no requirement to pursue the full 100 generations, given the satisfactory results obtained.

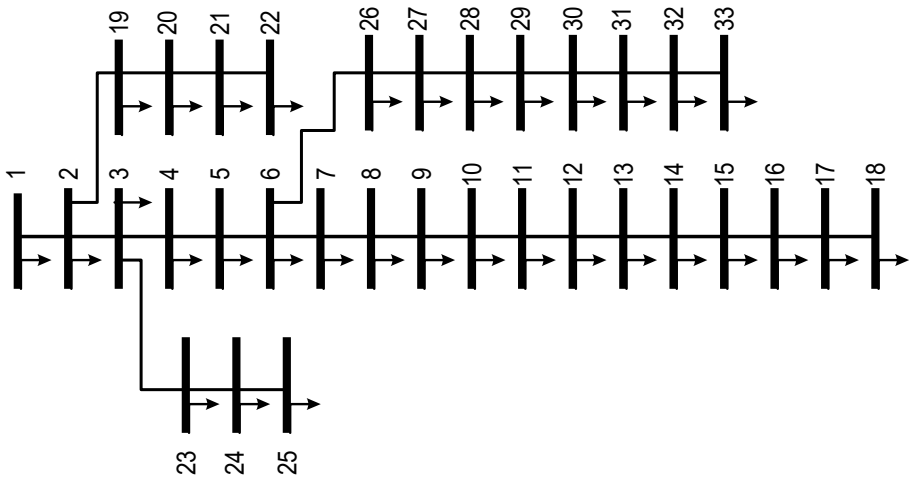


Figure 2. One-line diagram for the IEEE 33-bus network.

Table 1. Optimal PVDG allocations on the IEEE 33-bus network.

PVDG Size (kW)	Location
532	25
866	33
833	13

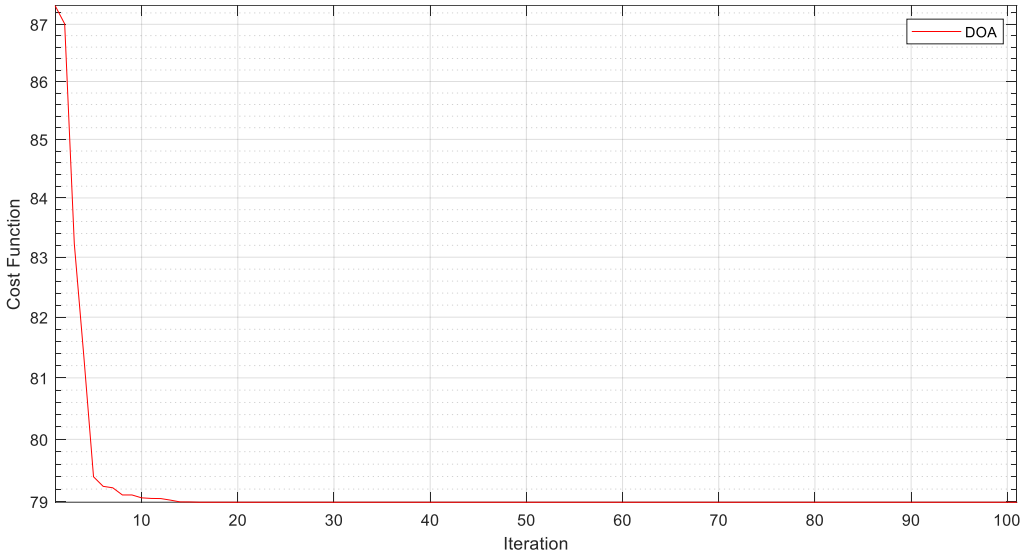


Figure 3. DOA convergence curve for PVDG allocation on the IEEE 33-bus network.

The subsequent subsections provide a comprehensive analysis of the DOA-optimized PVDG allocation impact on key parameters such as the voltage profile and active and reactive losses in the DN under the three loading conditions considered in this study.

4.1.1. Voltage Profile under Normal, Light, and Heavy Loads

Figure 4 presents the DN voltage profile under normal load conditions, comparing scenarios with and without the deployment of PVDG units. Before the integration of PVDG units, the voltage profile was found to be suboptimal, with multiple bus voltage magnitudes falling below the lower permissible limit of 0.95 p.u. Notably, buses 7 to 18 exhibited voltage magnitudes below this threshold, with bus 18 recording the lowest value at 0.9131 p.u. This indicates a subpar voltage profile in the network. However, after the strategic deployment of PVDG units, significant improvements were observed in the voltage magnitudes of these buses. Bus 30, in particular, achieved an impressive voltage value of 0.966 p.u., making a notable contribution to the overall enhancement of the network's voltage profile. These results demonstrate the effectiveness of DOA-optimized PVDG units in bolstering the network's voltage levels.

Furthermore, this study extended its investigation to scenarios with light and heavy loads, as shown in Figures 5 and 6, respectively. Under light load conditions (Figure 5), the voltage profile experienced a substantial boost due to PVDG deployment. The minimum voltage magnitude at bus 18 increased significantly from 0.9583 to 1.0096 p.u., which is well within the acceptable voltage limits of 0.95–1.05 p.u. The maximum voltage of 1.0131 p.u. was observed at bus 13 after PVDG deployment. Similarly, all other buses also saw a notable rise in voltage magnitudes. This demonstrates the versatility of the optimized PVDG units in enhancing the network's performance even under varying load conditions. Moreover, under heavy load conditions (Figure 6), the benefits of PVDG integration are even more pronounced. The minimum voltage magnitude improved from 0.9035 to 0.96004 p.u., representing an impressive 6.26% increase. The minimum voltage of 0.9582 p.u. occurred at bus 30 after the deployment of the DOA-optimized PVDG units. These findings underscore

the importance of the deployment of DOA-optimized PVDG units in mitigating voltage drop issues during periods of high demand. Under heavy load conditions, before the incorporation of PVDG units, the network's voltage profile suffered due to the heavy load it experienced. However, the successful deployment of PVDG units, optimized using a state-of-the-art method called the DOA, significantly improved the overall voltage profile. This optimization approach proves to be highly effective in determining the optimal allocation of PVDG units on radial DNs, as demonstrated in the results of this research. Thus, this study illustrates the significant positive impact of PVDG units on DNs' voltage profiles under normal, light, and heavy load conditions, as shown in Figures 4–6. The use of DOA for PVDG allocation showcases promising results, providing valuable insights into the practical enhancement of power DNs with PVDG integration.

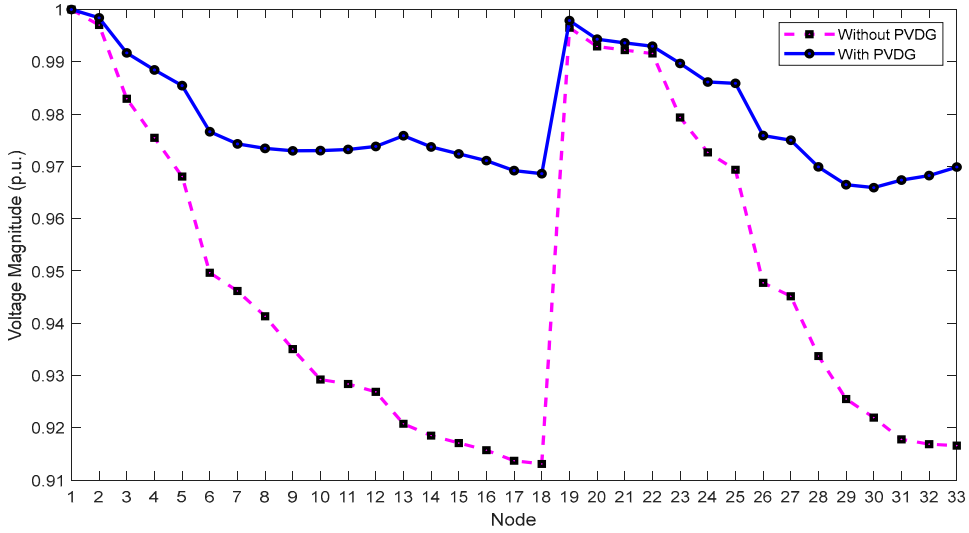


Figure 4. Voltage profile without and with PVDG placement under normal loads.

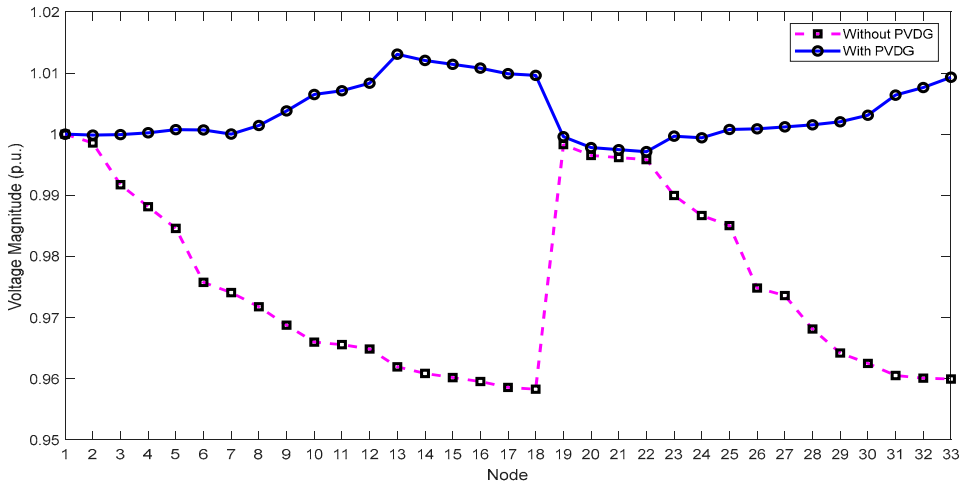


Figure 5. Voltage profile without and with PVDG placement under light loads.

Figure 7 depicts the voltage profile of the IEEE 33-bus network under base case conditions as well as voltage profiles under normal, light, and heavy loading scenarios subsequent to the integration of DOA-optimized PVDG units. This graphical exposition serves to substantiate the efficacy of DOA in the optimal allocation of PVDG units, thereby augmenting network performance across varying load conditions. Examining Figure 7, it becomes evident that the voltage profiles across the network under varied loading conditions, subsequent to the implementation of DOA-optimized PVDG units, remain

compliant with the stipulated voltage limits of 0.95–1.05 p.u. This observation serves to reinforce the assertion.

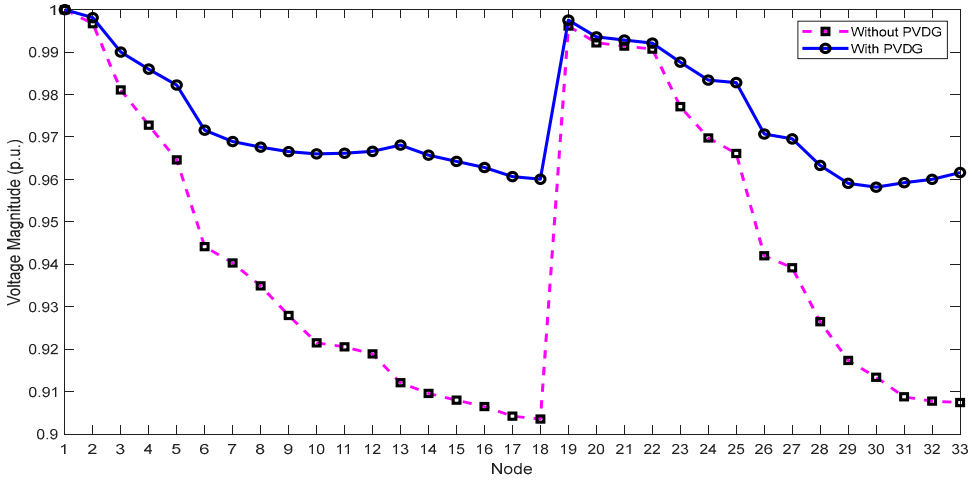


Figure 6. Voltage profile without and with PVDG placement under heavy loads.

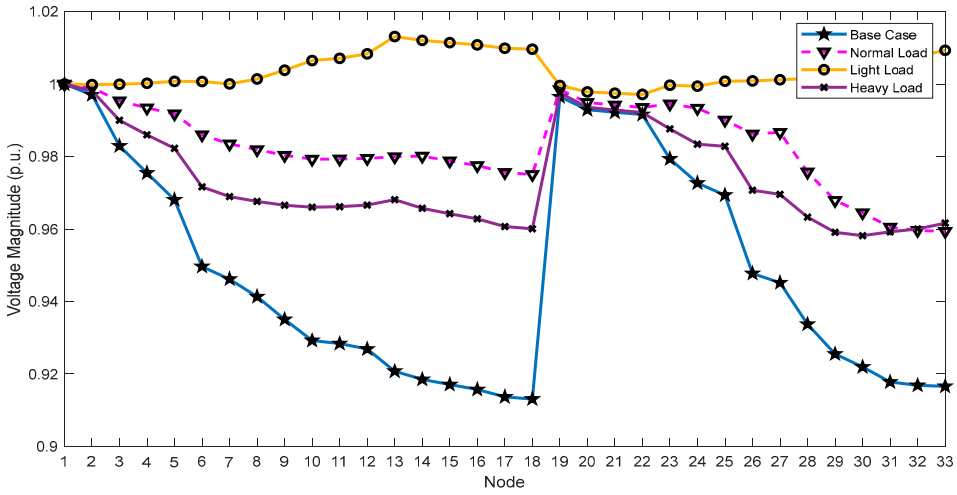


Figure 7. Voltage profile of the IEEE 33-bus network under different load conditions.

4.1.2. Active Power Loss under Normal, Light, and Heavy Loads

Figure 8 illustrates the total active power losses under normal, light, and heavy load conditions without and with PVDG deployment on the IEEE 33-bus network. As shown in Figure 8, prior to the implementation of PVDG units, the radial DN experienced an overall active power loss of 202.71 kW under normal loading conditions. However, using the DOA optimization algorithm for the strategic allocation of PVDG units, a remarkable reduction of 61.21% in total active power loss was achieved, equivalent to 78.62 kW. Figure 9 visually represents the distribution of active power losses across the network branches. Notably, the analysis of Figure 9 highlights that branch 2–3 exhibited the highest active power loss of 52 kW before the integration of the DOA-optimized PVDG units. However, with the optimal placement of PVDG units, this loss was significantly reduced to 14.95 kW, representing a substantial 71.25% reduction. The positive impact of the PVDG units was not limited to branch 2–3; there were significant reductions in active power losses observed in all the DN lines, leading to an overall enhancement in network efficiency. These reductions in individual branch losses collectively contributed to the substantial reduction in overall active power loss achieved across the entire network.

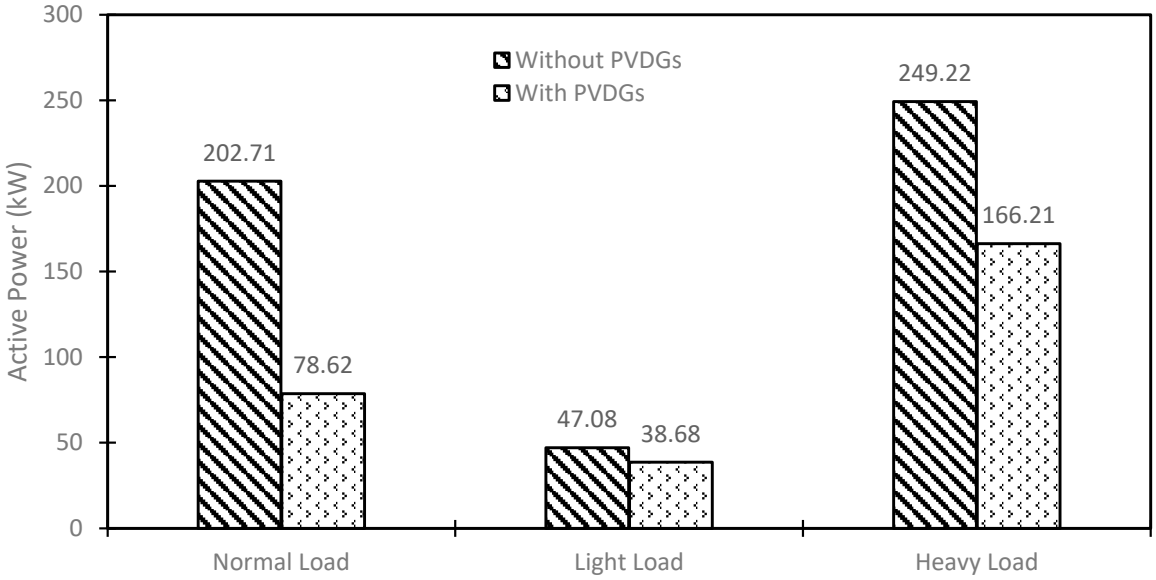


Figure 8. Total active power losses without and with PVDG placement under different load conditions.

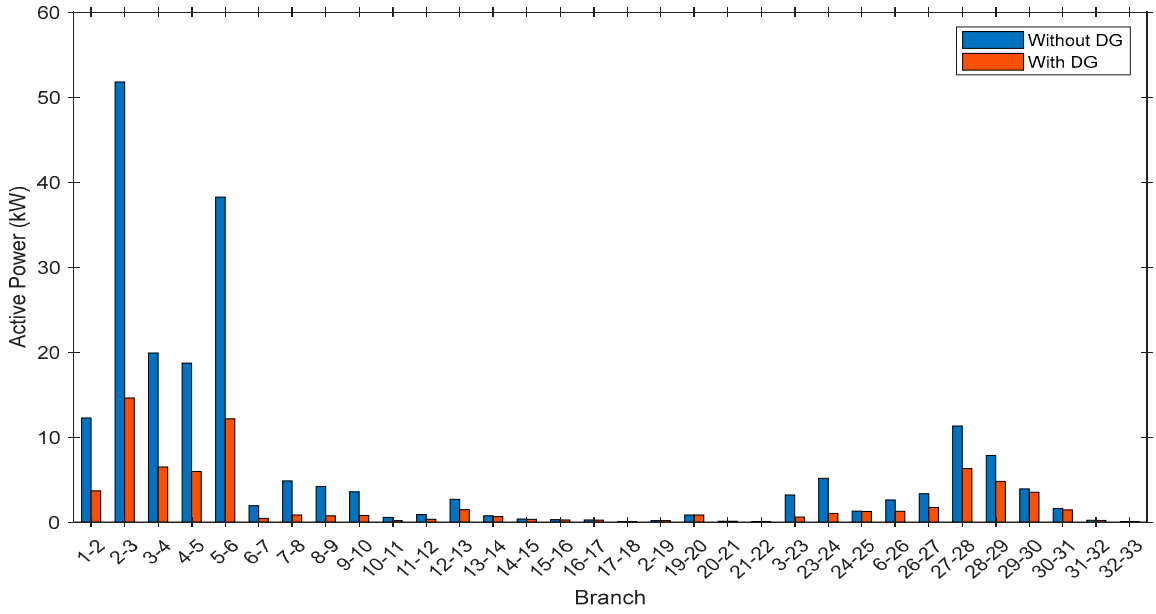


Figure 9. Active power losses across all the branches without and with PVDG placement under normal load conditions.

Additionally, even under light load conditions, as illustrated in Figure 8, the overall active power loss was significantly reduced from 47.08 to 38.68 kW, corresponding to an impressive 17.84% reduction in active power loss. This outcome was consistent with what was observed during normal loading conditions, where a remarkable decrease in overall active power loss in the network was evident due to the optimized allocation of PVDG units using the DOA technique. Figure 10 provides a comparative view of the active power losses across all network branches under light load conditions, both with and without the DOA-optimized PVDG deployment. Once again, branch 2–3 exhibited the highest active power loss among all the branches in the network, but after optimal PVDG deployment, these losses were significantly reduced.

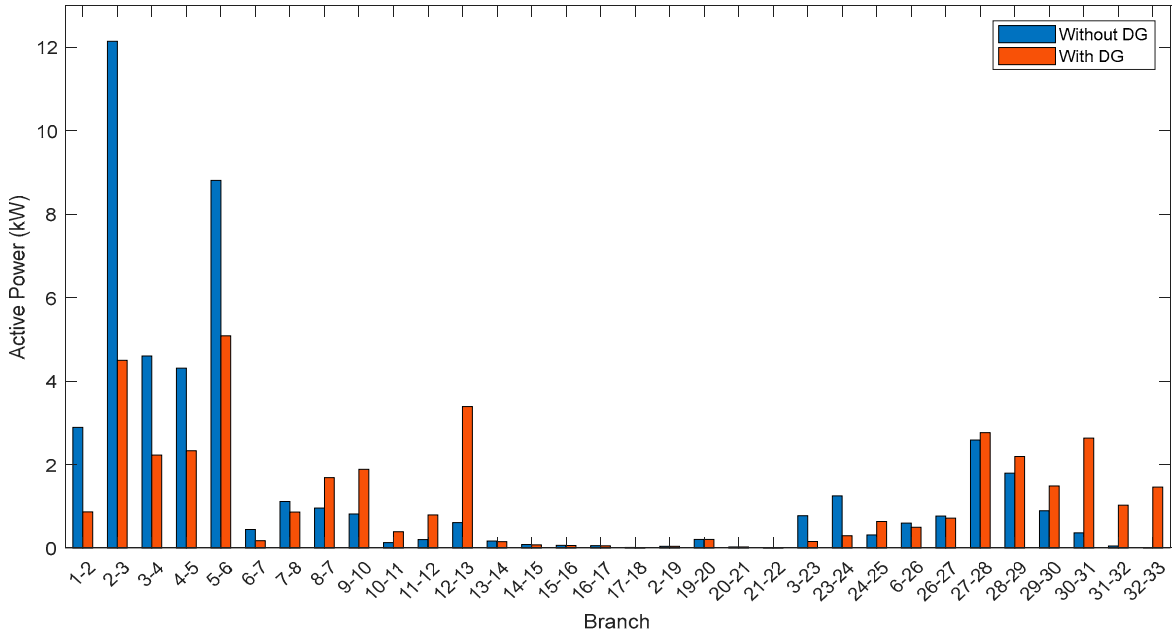


Figure 10. Active power losses across all the branches without and with PVDG placement under light load conditions.

Furthermore, the effectiveness of the DOA-optimized PVDGs was evident even under heavy load conditions. According to Figure 8, the total active power loss, which amounted to 249.22 kW, was remarkably minimized to 166.21 kW, corresponding to a 33.31% reduction, showcasing the efficacy of the DOA-optimized PVDG units in reducing total active power loss in the radial DN under heavy load conditions. Figure 11 illustrates the active power losses across all network branches under heavy load conditions, both with and without PVDG deployment, demonstrating how active power losses in all branches decrease with DOA-deployed PVDG units. Thus, the strategic allocation of PVDG units using the DOA proved to be highly effective in improving network performance under various load conditions. The results shown in Figures 9–11 underscore the efficacy and powerful characteristics of the DOA in enhancing network efficiency and reducing overall active power losses. This study represents a significant advancement in the field of radial DN optimization, showcasing the potential benefits of DOA-optimized PVDG integration in real-world applications.

4.1.3. Reactive Power under Normal, Light, and Heavy Loads

Figure 12 depicts the total reactive power losses in various scenarios, including normal, light, and heavy load conditions, both with and without the integration of PVDG on the IEEE 33-bus network. According to Figure 12, the total reactive power loss, initially at 23.56 kVAr, was significantly minimized to 10 kVAr, corresponding to an impressive 57.6% reduction. These findings affirm the remarkable performance enhancement achieved using the DOA in optimizing PVDG allocation. Similarly, Figure 13 presents a comparative analysis of reactive power losses across all branches in the DN before and after the strategic deployment of PVDGs under normal operating conditions. Initially, branches 2–3 and 5–6 exhibited the highest reactive power losses, amounting to 26 kVAr and 34 kVAr, respectively. However, after optimizing the allocation of PVDGs using a novel DOA, these losses were substantially minimized to 7 and 11 kVAr, respectively. This compellingly demonstrates the effectiveness of strategically allocated PVDGs in mitigating reactive power losses across all branches of the DN under study. Furthermore, Figure 13 indicates a general reduction in reactive losses throughout the DN branches.

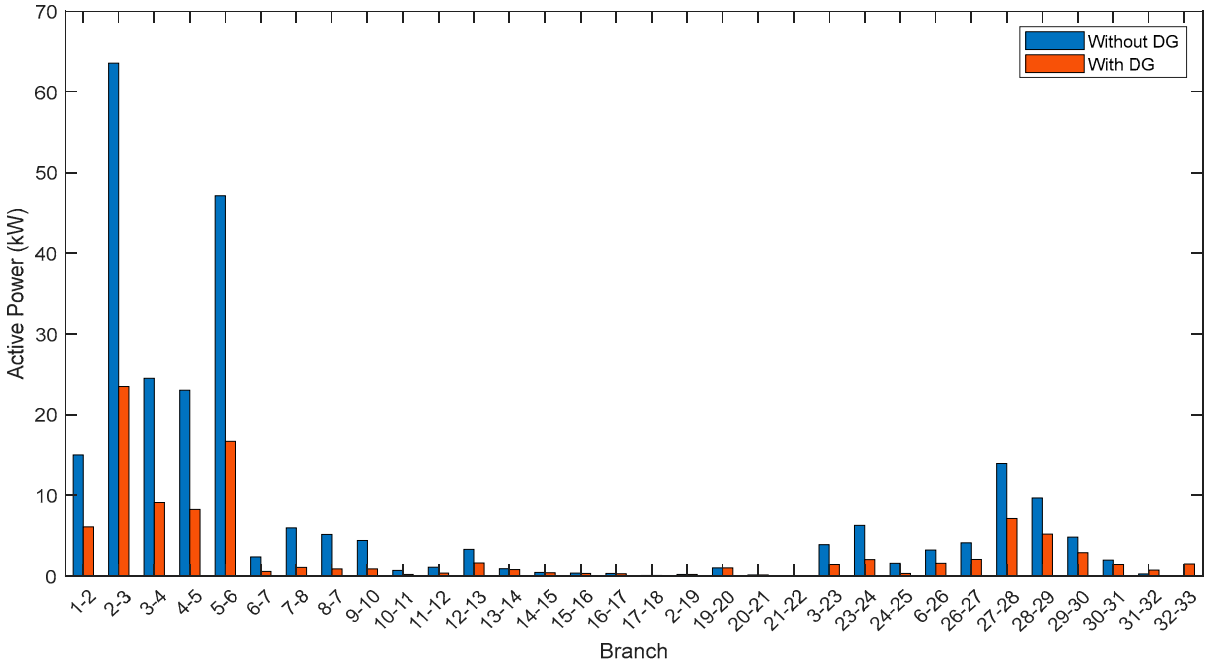


Figure 11. Active power losses across all branches without and with PVDG placement under heavy load conditions.

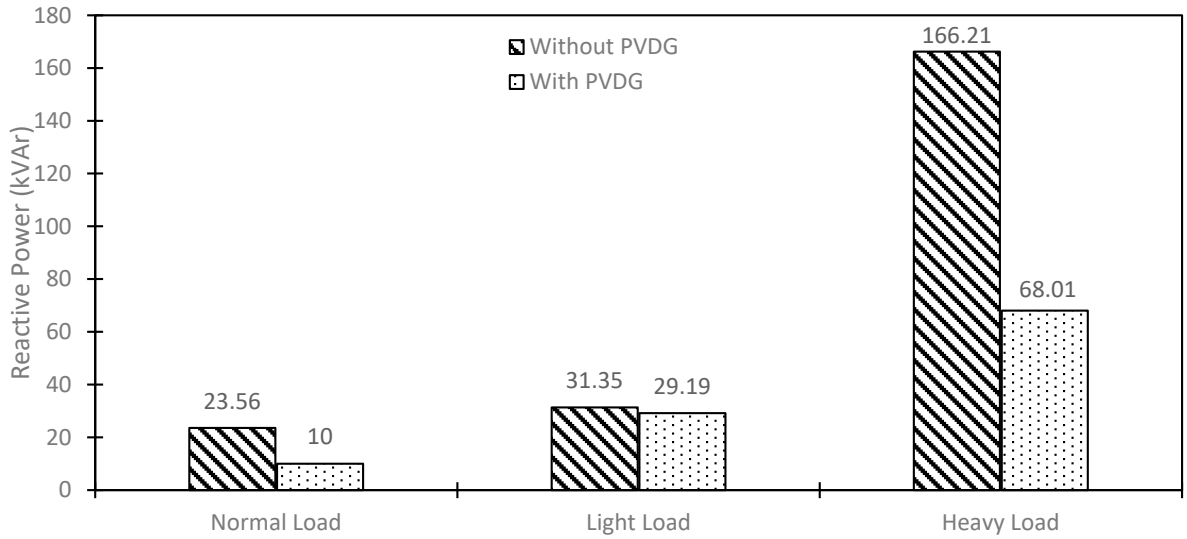


Figure 12. Total reactive power losses without and with PVDG placement under different load conditions.

Under light load conditions, according to Figure 12, the total reactive power loss in the network, originally at 31.35 kVAr, was remarkably reduced to 29.19 kVAr, corresponding to a substantial 6.89% reduction. Similarly, under light loading conditions, as depicted in Figure 14, the implementation of DOA-optimized PVDGs led to a substantial reduction in reactive power losses across all network branches. Notably, this reduction was most pronounced in branches 2–3 and 5–6, which exhibited the highest levels of reactive power losses among all the network buses without PVDG deployment. This trend continued across the remaining network branches, as illustrated in Figure 14, further underscoring the efficiency of the DOA-optimized PVDG units in minimizing reactive power losses throughout the network.

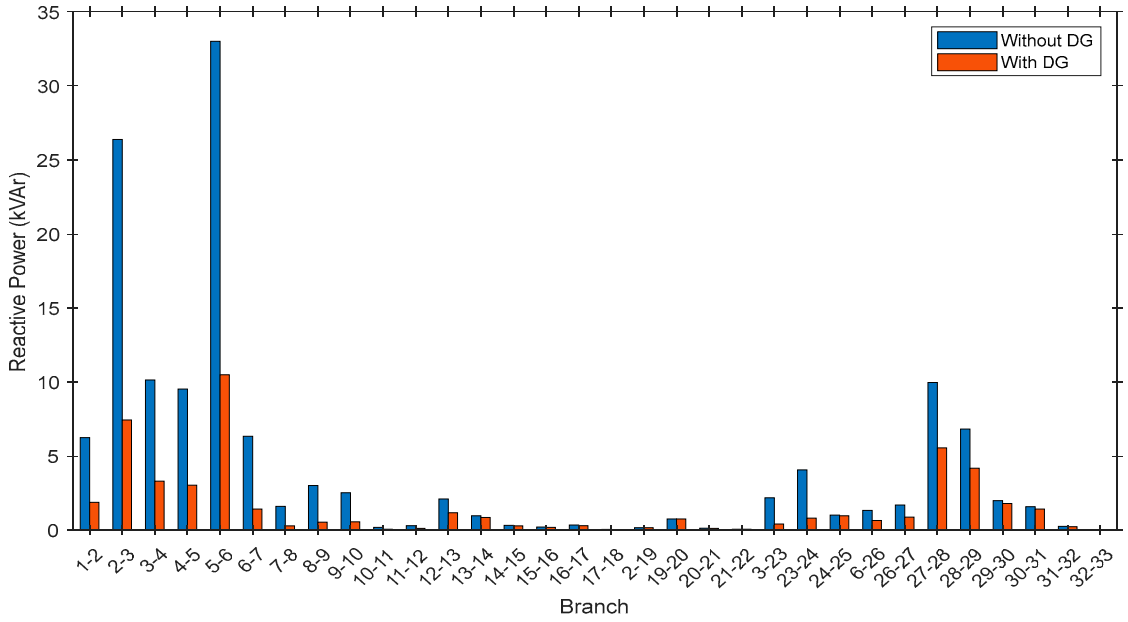


Figure 13. Reactive power losses across all branches without and with PVDG placement under normal load conditions.

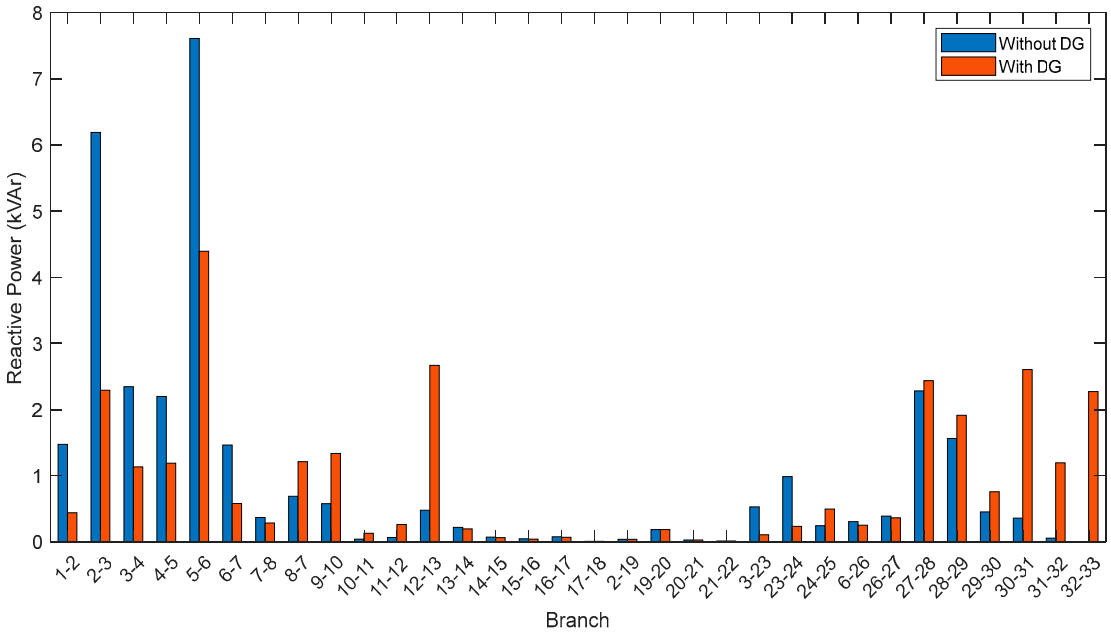


Figure 14. Reactive power losses across all branches without and with PVDG placement under light load conditions.

Under heavy load conditions, as also depicted in Figure 12, the total reactive power loss, initially at 166.21 kVAr, was impressively reduced to 68.01 kVAr, corresponding to an outstanding 59.03% reduction. As depicted in Figure 15, similar to previous scenarios, branches 2–3 and 5–6 exhibited the highest reactive power losses, but following the deployment of DOA-optimized PVDGs, these losses experienced a significant reduction. Reactive power losses across all network branches also witnessed noteworthy decreases after the deployment of DOA-optimized PVDG units, further validating the effectiveness of DOA in optimizing PVDG units within radial DNs.

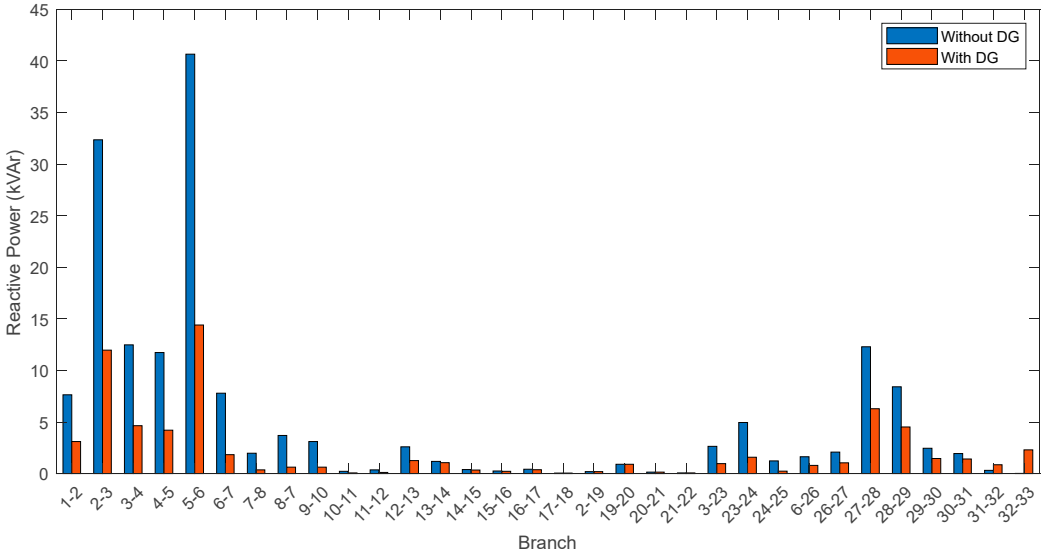


Figure 15. Reactive power losses across all branches without and with PVDG placement under heavy load condition.

Therefore, Figures 13–15 collectively demonstrate the remarkable efficacy of the DOA in strategically allocating PVDG units to substantially reduce reactive power losses in radial DNs. These findings have significant implications for enhancing the overall performance and efficiency of DNs and contributing to a more sustainable and reliable power infrastructure.

4.2. Ajinde 62-Bus Network

This particular DN comprises 62 buses and 61 lines. The bus and line data of this network were sourced from the Ibadan Electricity Distribution Company of Nigeria (IBEDC) as shown in Tables A1 and A2, respectively in Appendix A. The total active load and reactive load on the network were recorded as 2.07 MW and 1.29 MVAr, respectively, with a nominal voltage of 11 kV. This network is one of the radial DNs owned by IBEDC in Nigeria. To visually represent the network configuration, Figure 16 presents a single-line diagram. In this study, three PVDG units were strategically deployed on this DN to assess the DOA algorithm's effectiveness in allocating them, with the aim of improving network performance and enhancing its resilience against voltage collapse.

The power flow simulation converged after three iterations, and the resulting simulation outcomes are documented in Table 2. Using PVDG optimization, it was determined that buses 17, 27, and 33 were the optimal locations for the placement of PVDG units. Table 2 provides details of the recommended PVDG unit sizes for these buses, which were obtained as 757, 150, and 1097 kW, respectively. The DOA convergence curve is depicted in Figure 17. Similarly, as in the case of the simulation for the IEEE 33-bus DN, convergence was achieved after about 21 iterations, despite the maximum limit being set at 100, which further emphasizes the efficacy of DOA. The subsequent subsections present a comprehensive analysis of the impact of PVDG allocations on critical network parameters such as the voltage profile and active and reactive losses within the DN.

Table 2. Optimal PVDG allocations on the Ajinde 62-bus network.

PVDG Size (kW)	Location
757	17
150	27
1097	33

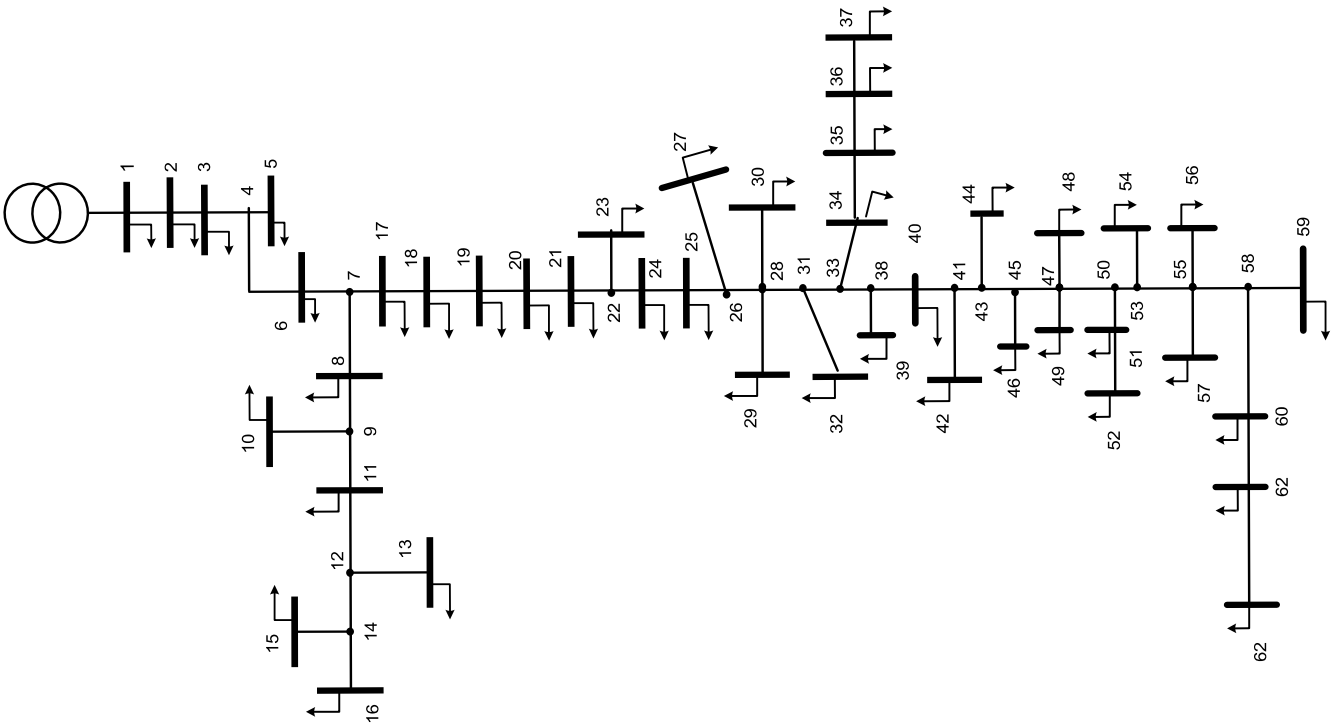


Figure 16. One-line diagram for the Ajinde 62-bus network.

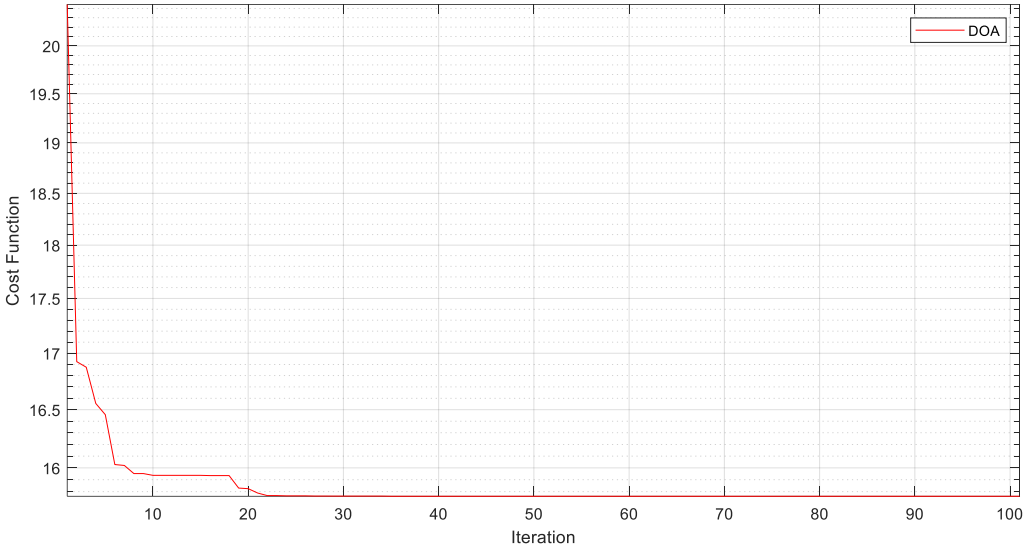


Figure 17. DOA convergence curve for PVDG allocation on the Ajinde 62-bus network.

4.2.1. Voltage Profile

Figure 18 shows the voltage profile of the test network without and with the integration of PVDG units. Initially, the voltage profile was considered satisfactory since all buses maintained voltage levels within the allowable limits of 0.95–1.05 p.u. However, the network may exhibit vulnerability to sudden load increases, potentially causing an unfavorable voltage profile, as several buses operated slightly above the minimum voltage limit of 0.95 p.u. Upon the optimal deployment of PVDGs, the voltage magnitudes of buses that previously hovered just above the lower voltage limit witnessed a significant improvement. Notably, Bus 62, which initially registered a voltage magnitude of 0.9533 p.u., experienced a substantial increase to 0.97501 p.u. The rest of the buses in the network also displayed remarkable enhancements in their voltage magnitudes, leading to an overall

improvement in the DN's voltage profile. This remarkable enhancement was achieved using an innovative DOA approach, as highlighted in Figure 18. DOA played a crucial role in efficiently sizing and placing the PVDG units within the network, effectively mitigating potential voltage issues, and reinforcing the network against load fluctuations. Overall, the integration of PVDG units and the bio-inspired DOA-based optimization process resulted in a significantly improved and robust voltage profile for the test network, paving the way for a more stable and reliable DN.

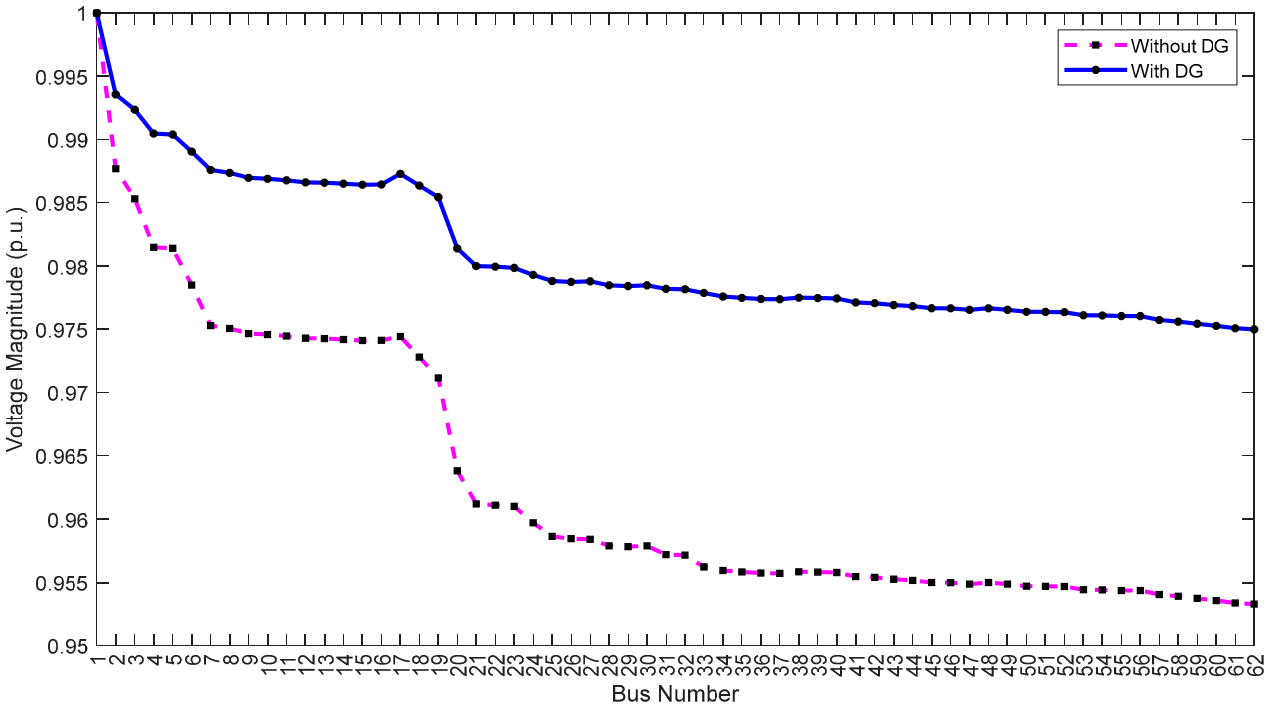


Figure 18. Voltage profile without and with PVDG placement.

4.2.2. Active Power Loss

Before the integration of PVDG units into the network, the total active power loss amounted to 52.17 kW. However, by strategically implementing the DOA to allocate PVDG units, a remarkable reduction of 71.05% in total active power loss was achieved, resulting in a significant decrease of 15.104 kW. Figure 19 graphically represents the impact of this optimization, displaying the active losses in all the DN branches both before and after the deployment of PVDG units.

Upon careful examination of Figure 19, it becomes evident that the maximum active power loss of 17.57 kW, which occurred in branch 1–2 of the test network without PVDG units, was impressively reduced to 4.762 kW after the optimal deployment of PVDG units. This represents a substantial 73% decrease in active power loss for this particular branch. Moreover, this successful integration of PVDGs led to a significant reduction in active power losses across all branches of the test network, resulting in an overall enhancement of the network's efficiency. This indicates that the DOA's strategic placement of PVDG units had a positive impact on the network's performance, leading to improved energy conservation and better utilization of resources.

4.2.3. Reactive Power

Figure 20 presents a comparative analysis of reactive losses in all DN branches pre- and post-allocation of PVDG units. An examination of Figure 20 emphasizes that branches 1–2 and 19–20 exhibited the highest initial reactive power losses, measuring 30.11 and 12.07 kVAr, respectively. However, using optimal PVDG allocation, these losses were significantly reduced to 8.06 and 3.23 kVAr, respectively. This exemplifies the remarkable

effectiveness of strategically allocated PVDGs in mitigating reactive power losses across all DN branches. Furthermore, Figure 20 indicates widespread reductions in reactive losses throughout the DN branches. Consequently, the total reactive loss, initially recorded at 88.07 kVAr, experienced a significant reduction to 24.20 kVAr, corresponding to an impressive 72.52% decrease. These findings unequivocally affirm the proficiency of the DOA methodology in optimizing PVDG allocation to enhance the performance of DNs.

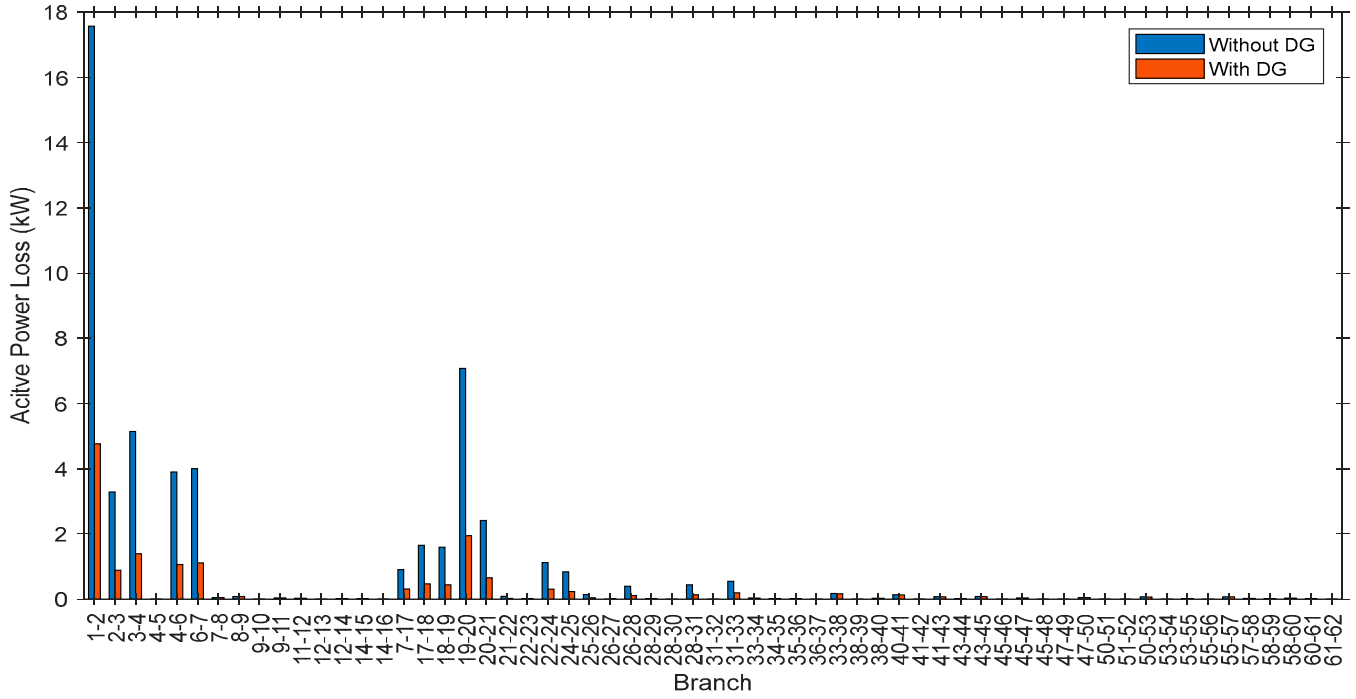


Figure 19. Active power losses across all branches without and with PVDG placement.

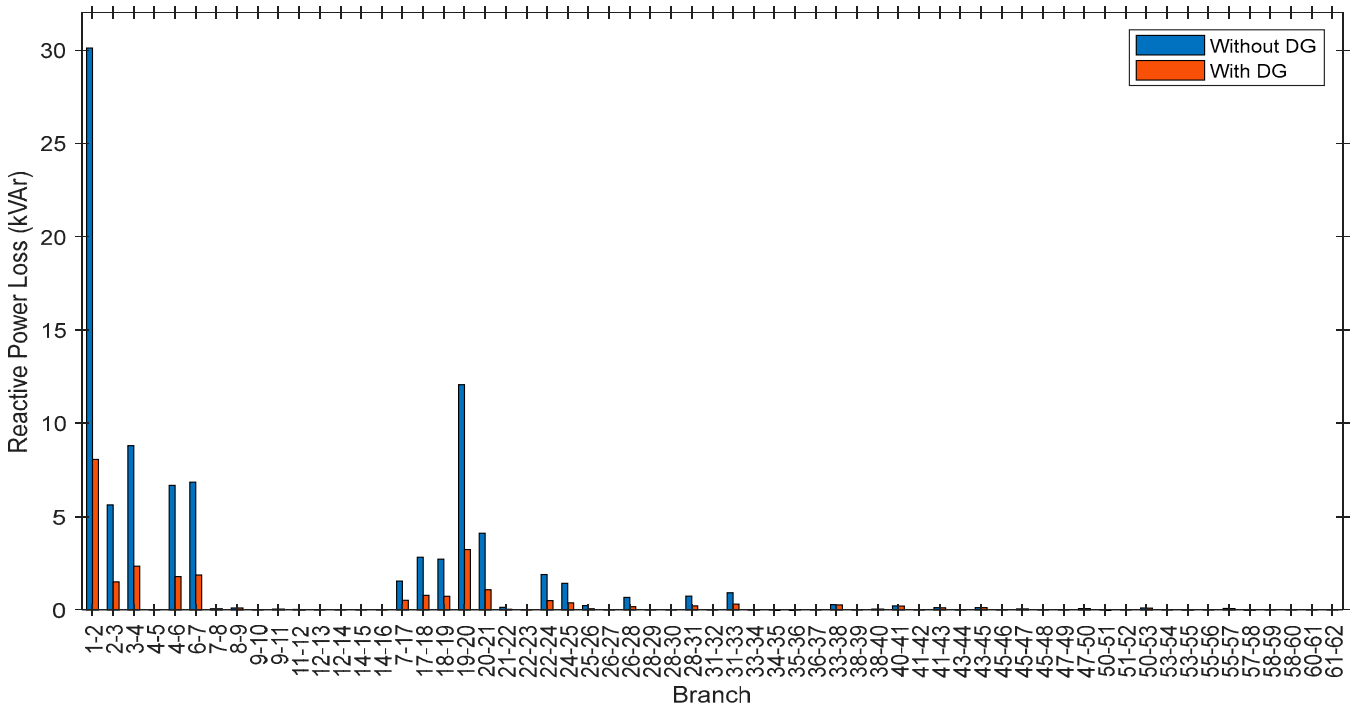


Figure 20. Reactive power losses across all branches without and with PVDG placement.

4.3. Comparison with Other Metaheuristic Optimization Algorithms

In the assessment of DOA's effectiveness, a comprehensive evaluation was conducted by comparing it with other well-established bio-inspired optimization algorithms documented in the existing literature. This investigation was carried out on the IEEE 33-bus network, providing a solid basis for analysis. The findings of this comparative study are concisely summarized in Table 3. The results showcase the remarkable performance of the proposed DOA, as it achieved the highest reduction in power losses, demonstrating an impressive decrease of 61.21%. Notably, the ABC algorithm also exhibited significant effectiveness with a reduction of 61.13% in power losses, and the LSFSA performed commendably, yielding a reduction of 61.10%. These outcomes underscore the competitive nature of the proposed DOA, positioning it as the superior choice among the bio-inspired optimization algorithms examined in the existing literature, as indicated by the results presented in Table 3. Such substantial power loss reduction highlights the potential of the DOA in optimizing PVDG units to contribute significantly to power system efficiency and sustainability.

Table 3. Comparison among the proposed DOA and other optimization algorithms.

Method	Optimal Location	DG Size (MW)	Loss Reduction (kW)	Loss Reduction (%)
ABC [26]	6, 15, 25	1.75, 0.57, 0.78	79.25	61.13
WAO [27]	14, 24, 31	1.02, 1.20, 1.20	79.72	60.67
GA/PSO [28]	32, 16, 11	1.20, 0.86, 0.93	99.33	50.99
BFOA [29]	14, 18, 32	0.65, 0.19, 0.11	86.38	57.38
PSO [28]	13, 32, 8	0.98, 0.83, 1.18	101.21	50.06
LSFSA [30]	6, 18, 30	1.11, 0.49, 0.87	82.03	61.10
GA [28]	11, 29, 30	1.50, 0.42, 1.07	104.6	49.60
FA [31]	13, 17, 31	0.62, 0.26, 0.10	87.83	58.37
DOA	13, 25, 33	0.53, 0.87, 0.83	78.62	61.21

5. Conclusions

This study's findings reveal valuable insights into the optimal allocation of PVDGs to enhance the performance of two different DNs: the IEEE 33-bus DN and the Ajinde 62-bus DN. For the IEEE 33-bus DN, the research identified specific buses that proved to be optimal locations for PVDGs. Buses 13, 25, and 33 were deemed the best locations for PVDG installation and the appropriate sizes were determined to be 833, 532, and 866 kW, respectively. Similarly, for the Ajinde 62-bus DN, this study identified buses 17, 27, and 33 as the best locations for PVDGs, with respective optimal sizes of 757, 150, and 1097 kW, respectively. The implementation of the optimal PVDG allocation resulted in significant improvements in the performance of both DNs. For the IEEE 33-bus DN, the smallest voltage magnitude increased to 0.966 p.u. under normal loading conditions, 1.0096 p.u. under light loading conditions, and 0.96004 p.u. under heavy loading conditions. Additionally, active power reductions of 61.21, 17.84, and 33.31% were achieved, respectively, indicating enhanced network efficiency and reduced power losses. Similarly, for the Ajinde 62-bus DN, the smallest voltage magnitude reached 0.9787 p.u., and the total active power loss was reduced by an impressive 71.05%. Furthermore, a comparative analysis with other optimization techniques documented in the literature further substantiated the superior performance of DOA in effectively allocating PVDGs. Thus, the findings demonstrate the remarkable effectiveness of the DOA in strategically allocating PVDGs to improve the performance of DNs under different loading conditions. By identifying the optimal locations and sizes of PVDGs, the DOA offers an efficient approach to enhancing network stability, minimizing power losses, and paving the way for more sustainable and resilient power distribution systems. However, there is a need for further research to incorporate variations in the output of PVDGs when applying the DOA for allocation, especially considering the hybridization of the DOA to solve more complex objective functions, particularly for large-scale systems. Accounting for these variations is crucial to enhancing the algorithm's effectiveness in real-world scenarios and ensuring accurate and reliable PVDG placements on distribution networks.

Author Contributions: Conceptualization, S.O.A. and F.K.A.; methodology, S.O.A., F.K.A., K.T.A. and A.J.; software, S.O.A., E.I.O. and D.E.O.; validation, S.O.A., K.T.A. and A.J.; formal analysis, S.O.A. and F.K.A.; investigation, S.O.A., A.J. and A.O.A.; resources, S.O.A. and F.K.A.; data curation, S.O.A. and A.J.; writing—original draft preparation, S.O.A.; writing—review and editing, S.O.A., F.K.A. and K.T.A.; visualization, S.O.A., F.K.A., A.J., E.I.O., D.E.O. and A.O.A.; supervision, F.K.A. and K.T.A.; project administration, S.O.A. and F.K.A.; funding acquisition, K.T.A. and A.J. All authors have read and agreed to the published version of the manuscript.

Funding: This research received no external funding.

Institutional Review Board Statement: Not applicable.

Informed Consent Statement: Not applicable.

Data Availability Statement: The bus and line data for the Ajinde 62-bus network were obtained from Ibadan Electricity Distribution Company, Nigeria.

Conflicts of Interest: The authors declare no conflict of interest.

Appendix A

Table A1. Bus Data for the Ajinde 62-Bus Network (IBEDC).

Bus No	P (kW)	Q (kVAr)
1	0	0
2	70.448	43.9264
3	63.648	39.6864
4	0	0
5	52.088	32.4784
6	86.02	53.636
7	0	0
8	4.352	2.7136
9	0	0
10	39.032	24.3376
11	47.668	29.7224
12	0	0
13	72.76	45.368
14	0	0
15	67.524	42.1032
16	65.96	41.128
17	41.004	25.5672
18	75.888	47.3184
19	4.352	2.7136
20	61.2	38.16
21	94.112	58.6816
22	0	0
23	85.204	53.1272
24	19.108	11.9144
25	77.248	48.1664
26	0	0
27	35.36	22.048
28	23.324	14.5432
29	84.116	52.4488
30	13.328	8.3104
31	0	0
32	77.996	48.6328
33	0	0
34	39.848	24.8464
35	7.6704	4.782733
36	46.988	29.2984
37	71.876	44.8168
38	0	0

Table A1. *Cont.*

Bus No	P (kW)	Q (kVAr)
39	33.456	20.8608
40	24.82	15.476
41	0	0
42	74.528	46.4704
43	0	0
44	75.344	46.9792
45	0	0
46	20.0804	12.520733
47	0	0
48	9.991933	6.230267
49	0.5372	0.334967
50	0	0
51	2.9784	1.8571
52	49.98	31.164
53	0	0
54	30.872	19.2496
55	0	0
56	1.9584	1.221133
57	92.208	57.4944
58	0	0
59	93.908	58.5544
60	68.748	42.8664
61	38.488	23.9984
62	26.18	16.324

Table A2. Line and Bus Data for the Ajinde 62-Bus Network (IBEDC).

from Bus	to Bus	Length (km)	R (Ω)	X (Ω)	1/2 B (S)
1	2	1.5	0.273750	0.471300	1.37×10^{-6}
2	3	0.3	0.054750	0.094260	2.73×10^{-7}
3	4	0.5	0.091250	0.157100	4.56×10^{-7}
4	5	0.4	0.073000	0.125680	3.64×10^{-7}
4	6	0.4	0.073000	0.125680	3.64×10^{-7}
6	7	0.45	0.082125	0.141390	4.10×10^{-7}
7	8	0.2	0.036500	0.062840	1.82×10^{-7}
8	9	0.35	0.063875	0.109970	3.19×10^{-7}
9	10	0.5	0.091250	0.157100	4.56×10^{-7}
9	11	0.2	0.036500	0.062840	1.82×10^{-7}
11	12	0.21	0.038325	0.065982	1.91×10^{-7}
12	13	0.1	0.018250	0.031420	9.11×10^{-8}
12	14	0.2	0.036500	0.062840	1.82×10^{-7}
14	15	0.32	0.058400	0.100544	2.92×10^{-7}
14	16	0.25	0.045625	0.078550	2.28×10^{-7}
7	17	0.145	0.026463	0.045559	1.32×10^{-7}
17	18	0.28	0.051100	0.087976	2.55×10^{-7}
18	19	0.3	0.054750	0.094260	2.73×10^{-7}
19	20	1.34	0.244550	0.421028	1.22×10^{-6}
20	21	0.5	0.091250	0.157100	4.56×10^{-7}
21	22	0.02	0.003650	0.006284	1.82×10^{-8}
22	23	0.3	0.054750	0.094260	2.73×10^{-7}
22	24	0.31	0.056575	0.097402	2.82×10^{-7}
24	25	0.24	0.043800	0.075408	2.19×10^{-7}
25	26	0.045	0.008213	0.014139	4.10×10^{-8}
26	27	0.35	0.063875	0.109970	3.19×10^{-7}
26	28	0.14	0.025550	0.043988	1.28×10^{-7}

Table A2. *Cont.*

from Bus	to Bus	Length (km)	R (Ω)	X (Ω)	1/2 B (S)
28	29	0.2	0.036500	0.062840	1.82×10^{-7}
28	30	0.05	0.009125	0.015710	4.56×10^{-8}
28	31	0.2	0.036500	0.062840	1.82×10^{-7}
31	32	0.12	0.021900	0.037704	1.09×10^{-7}
31	33	0.3	0.054750	0.094260	2.73×10^{-7}
33	34	0.44	0.080300	0.138248	4.01×10^{-7}
34	35	0.21	0.038325	0.065982	1.91×10^{-7}
35	36	0.2	0.036500	0.062840	1.82×10^{-7}
36	37	0.075	0.013688	0.023565	6.83×10^{-8}
33	38	0.15	0.027375	0.047130	1.37×10^{-7}
38	39	0.19	0.034675	0.059698	1.73×10^{-7}
38	40	0.025	0.004563	0.007855	2.28×10^{-8}
40	41	0.14	0.025550	0.043988	1.28×10^{-7}
41	42	0.2	0.036500	0.062840	1.82×10^{-7}
41	43	0.102	0.018615	0.032048	9.29×10^{-8}
43	44	0.3	0.054750	0.094260	2.73×10^{-7}
43	45	0.15	0.027375	0.047130	1.37×10^{-7}
45	46	0.1	0.018250	0.031420	9.11×10^{-8}
45	47	0.08	0.014600	0.025136	7.29×10^{-8}
45	48	0.06	0.010950	0.018852	5.47×10^{-8}
47	49	0.245	0.044713	0.076979	2.23×10^{-7}
47	50	0.1	0.018250	0.031420	9.11×10^{-8}
50	51	0.04	0.007300	0.012568	3.64×10^{-8}
51	52	0.1	0.018250	0.031420	9.11×10^{-8}
50	53	0.2	0.036500	0.062840	1.82×10^{-7}
53	54	0.15	0.027375	0.047130	1.37×10^{-7}
53	55	0.05	0.009125	0.015710	4.56×10^{-8}
55	56	0.35	0.063875	0.109970	3.19×10^{-7}
55	57	0.25	0.045625	0.078550	4.56×10^{-7}
57	58	0.15	0.027375	0.047130	2.73×10^{-7}
58	59	0.45	0.082125	0.141390	8.20×10^{-7}
58	60	0.65	0.118625	0.204230	1.18×10^{-6}
60	61	0.75	0.136875	0.235650	1.37×10^{-6}
61	62	0.85	0.155125	0.267070	1.55×10^{-6}

References

1. Ayanlade, S.O.; Komolafe, O.A. Distribution System Voltage Profile Improvement Based on Network Structural Characteristics. In Proceedings of the OAU Faculty of Technology Conference OAUTEKCONF 2019, Obafemi Awolowo University, Ile-Ife, Nigeria, 22–25 September 2019; pp. 75–80.
2. Mahdavi, E.; Asadpour, S.; Macedo, L.H.; Romero, R. Reconfiguration of Distribution Networks with Simultaneous Allocation of Distributed Generation Using the Whale Optimization Algorithm. *Energies* **2023**, *16*, 4560. [CrossRef]
3. Alanazi, A.; Alanazi, T.I. Multi-Objective Framework for Optimal Placement of Distributed Generations and Switches in Reconfigurable Distribution Networks: An Improved Particle Swarm Optimization Approach. *Sustainability* **2023**, *15*, 9034. [CrossRef]
4. Thang, V.V.; Trung, N.H. Evaluating efficiency of renewable energy sources in planning micro-grids considering uncertainties. *J. Energy Syst.* **2019**, *3*, 14–25. [CrossRef]
5. Reddy, G.H.; Koundinya, A.N.; Gope, S.; Singh, K.M. Optimal Sizing and Allocation of DG and FACTS Device in the Distribution System using Fractional Lévy flight BAT Algorithm. *IFAC-PapersOnLine* **2022**, *55*, 168–173. [CrossRef]
6. Bawazir, R.O.; Cetin, N.S. Comprehensive overview of optimizing PV-DG allocation in power system and solar energy resource potential assessments. *Energy Rep.* **2020**, *6*, 173–208. [CrossRef]
7. Janamala, V.; Radha Rani, K. Optimal Allocation of Solar Photovoltaic Distributed Generation in Electrical Distribution Networks using Archimedes Optimization Algorithm. *Clean Energy* **2022**, *6*, 271–287. [CrossRef]
8. Albadi, M.; Soliman, H.; Thani, M.A.; Al-Alawi, A.; Al-Ismaili, S.; Al-Nabhani, A.; Baalawi, H. Optimal allocation of PV systems to Minimize Losses in Distribution Networks using GA and PSO: Masirah Island Case Study. *J. Electr. Syst.* **2017**, *13*, 678–688.
9. Ali, E.S.; Abd Elazim, S.M.; Hakmi, S.H.; Mosaad, M.I. Optimal Allocation and Size of Renewable Energy Sources as Distributed Generations Using Shark Optimization Algorithm in Radial Distribution Systems. *Energies* **2023**, *16*, 3983. [CrossRef]

10. Khenissi, I.; Sellami, R.; Fakhfakh, M.A.; Neji, R. Power Loss Minimization Using Optimal Placement and Sizing of Photovoltaic Distributed Generation under Daily Load Consumption Profile with PSO and GA Algorithms. *J. Control Autom. Electr. Syst.* **2021**, *32*, 1317–1331. [CrossRef]
11. Albadi, M.H.; Soliman, H.M.; El-Saadany, E.F.; Thani, M.A.; Al-Alawi, A.; Al-Ismaili, S.; Baalawi, H. Optimal allocation of PV systems in distribution networks using PSO. In Proceedings of the 2017 7th International Conference on Modeling, Simulation, and Applied Optimization (ICMSAO), Sharjah, United Arab Emirates, 4–6 April 2017; IEEE: Piscataway, NJ, USA, 2017; pp. 1–5.
12. Ali, E.S.; Abd Elazim, S.M.; Abdelaziz, A.Y. Optimal Allocation and Sizing of Renewable Distributed Generation using Ant Lion Optimization Algorithm. *Electr. Eng.* **2018**, *100*, 99–109. [CrossRef]
13. Ahmed, I.M.; Kamel, S.; Abdel-Mawgoud, H.; Yu, J. Optimal allocation of PV based DG in distribution networks at different load levels. In Proceedings of the 2018 Twentieth International Middle East Power Systems Conference (MEPCON), Cairo, Egypt, 18–20 December 2018; IEEE: Piscataway, NJ, USA, 2018; pp. 649–654.
14. Ahmadi, M.; Lotfy, M.E.; Shigenobu, R.; Yona, A.; Senjyu, T. Optimal sizing and placement of rooftop solar photovoltaic at kabul city real distribution network. *IET Gener. Transm. Distrib.* **2018**, *12*, 303–309. [CrossRef]
15. Khasanov, M.; Kamel, S.; Halim Houssein, E.; Rahmann, C.; Hashim, F.A. Optimal allocation strategy of photovoltaic-and wind turbine-based distributed generation units in radial distribution networks considering uncertainty. *Neur. Comput. Appl.* **2023**, *35*, 2883–2908. [CrossRef]
16. Purlu, M.; Turkay, B.E. Optimal allocation of renewable distributed generations using heuristic methods to minimize annual energy losses and voltage deviation index. *IEEE Access* **2022**, *10*, 21455–21474. [CrossRef]
17. Tukkee, A.S.; Alali, M.J.; Zarkani, M.K. Applying a firefly algorithm for optimum allocation of solar photovoltaic units in a distribution system. In *IOP Conference Series: Materials Science and Engineering*; IOP Publishing: Bristol, UK, 2020; p. 012042. [CrossRef]
18. Mubarak, H.; Mansor, N.N.; Mokhlis, H.; Mohamad, M.; Mohamad, H.; Muhammad, M.A.; Samman, M.A.; Afzal, S. Optimum distribution system expansion planning incorporating DG based on N-1 criterion for sustainable system. *Sustainability* **2021**, *13*, 6708. [CrossRef]
19. Khan, M.H.; Ulasyar, A.; Khattak, A.; Zad, H.S.; Alsharef, M.; Alahmadi, A.A.; Ullah, N. Optimal sizing and allocation of distributed generation in the radial power distribution system using honey badger algorithm. *Energies* **2022**, *15*, 5891. [CrossRef]
20. Jamil Mahfoud, R.; Sun, Y.; Faisal Alkayem, N.; Haes Alhelou, H.; Siano, P.; Shafie-khah, M. A Novel Combined Evolutionary Algorithm for Optimal Planning of Distributed Generators in Radial Distribution Systems. *Appl. Sci.* **2019**, *9*, 3394. [CrossRef]
21. Nowdeh, S.A.; Davoudkhani, I.F.; Moghaddam, M.H.; Najmi, E.S.; Abdelaziz, A.Y.; Ahmadi, A.; Razavi, S.E.; Gandoman, F.H. Fuzzy multi-objective placement of renewable energy sources in distribution system with objective of loss reduction and reliability improvement using a novel hybrid method. *Appl. Soft Comput.* **2019**, *77*, 761–779. [CrossRef]
22. Bairwa, A.K.; Joshi, S.; Singh, D. Dingo optimizer: A nature-inspired metaheuristic approach for engineering problems. *Math. Probl. Eng.* **2021**, *2021*, 2571863. [CrossRef]
23. Ayanlade, S.O.; Jimoh, A.; Ezekiel, S.O.; Babatunde, A.A. Voltage Profile Improvement and Active Power Loss Reduction Through Network Reconfiguration Using Dingo Optimizer. In *ICACIn 2022 Advances on Intelligent Computing and Data Science*; Saeed, F., Mohammed, F., Mohammed, E., Al-Hadhrami, T., Al-Sarem, M., Eds.; Lecture Notes on Data Engineering and Communications Technologies; Springer: Cham, Switzerland, 2023; Volume 179. [CrossRef]
24. Ayanlade, S.O.; Jimoh, A.; Ogunwole, E.I.; Aremu, A.; Jimoh, A.B.; Owolabi, D.E. Simultaneous network reconfiguration and capacitor allocations using a novel dingo optimization algorithm. *Int. J. Electr. Comput. Eng. (IJECE)* **2023**, *13*, 2384–2395. [CrossRef]
25. Duong, M.Q.; Pham, T.D.; Nguyen, T.T.; Doan, A.T.; Tran, H.V. Determination of Optimal Location and Sizing of Solar Photovoltaic Distribution Generation Units in Radial Distribution Systems. *Energies* **2019**, *12*, 174. [CrossRef]
26. Lalitha, M.P.; Reddy, N.S.; Reddy, V.C.V. Optimal DG placement for maximum loss reduction in radial distribution system using abc algorithm. *Int. J. Rev. Comput.* **2010**, *3*, 44–52.
27. Kamel, S.; Selim, A.; Jurado, F.; Yu, J.; Xie, K.; Yu, C. Multi-objective whale optimization algorithm for optimal integration of multiple DGs into distribution systems. In Proceedings of the 2019 IEEE Innovative Smart Grid Technologies-Asia (ISGT Asia), Chengdu, China, 21–24 May 2019; pp. 1312–1317. [CrossRef]
28. Moradi, M.H.; Abedini, M. A combination of genetic algorithm and particle swarm optimization for optimal DG location and sizing in distribution systems. *Int. J. Electr. Power Energy Syst.* **2012**, *34*, 66–74. [CrossRef]
29. Kowsalya, M. Optimal size and siting of multiple distributed generators in distribution system using bacterial foraging optimization. *Swarm Evol. Comput.* **2013**, *15*, 58–65. [CrossRef]
30. Injeti, S.K.; Kumar, N.P. A novel approach to identify optimal access point and capacity of multiple DGs in a small, medium and large-scale radial distribution systems. *Int. J. Electr. Power Energy Syst.* **2013**, *45*, 142–151. [CrossRef]
31. Sudabattula, S.K.; Kowsalya, M. Optimal allocation of multiple distributed generators in distribution system using firefly algorithm. *J. Electr. Eng.* **2017**, *17*, 12.

Disclaimer/Publisher's Note: The statements, opinions and data contained in all publications are solely those of the individual author(s) and contributor(s) and not of MDPI and/or the editor(s). MDPI and/or the editor(s) disclaim responsibility for any injury to people or property resulting from any ideas, methods, instructions or products referred to in the content.